Phylogeography and subspecies revision of the hispid pocket mouse, *Chaetodipus hispidus* (Rodentia: Heteromyidae)

Author(s): John J. Andersen and Jessica E. Light
Source: Journal of Mammalogy, 93(4):1195-1215. 2012.
Published By: American Society of Mammalogists
DOI: http://dx.doi.org/10.1644/11-MAMM-A-341.3
URL: http://www.bioone.org/doi/full/10.1644/11-MAMM-A-341.3

Journal of Mammalogy, 93(4):1195–1215, 2012

Phylogeography and subspecies revision of the hispid pocket mouse, *Chaetodipus hispidus* (Rodentia: Heteromyidae)

John J. Andersen and Jessica E. Light*

Department of Wildlife and Fisheries Sciences, Texas A&M University, College Station, TX 77843, USA (JJA, JEL)

** Correspondent: jlight2@tamu.edu*

The hispid pocket mouse (*Chaetodipus hispidus*) is one of the most genetically and morphologically divergent species within the heteromyid genus *Chaetodipus*. Four subspecies of *C. hispidus* currently are recognized, *C. h. hispidus*, *C. h. paradoxus*, *C. h. spilotus*, and *C. h. zacatecae*, ranging from North Dakota south through the Great Plains and Texas to central Mexico. We investigated the phylogeographic structure within *C. hispidus* by examining mitochondrial DNA from both freshly collected and museum specimens from localities distributed throughout the range of the species. We also examined 11 cranial characters in 303 specimens to assess morphological variation within the species. Although morphometric analyses were unable to differentiate the subspecies, phylogenetic analyses of molecular data indicated that the 4 currently recognized subspecies of *C. hispidus* are not genetically distinct. Instead, our results indicate that there are 4 distinct mitochondrial clades of *C. hispidus* that do not correspond to the currently recognized subspecies, but whose geographic limits instead coincide with major geographical features in the southern United States and northern Mexico. The Southern Coahuila filter-barrier (Durango and Coahuila), the Deming Plains (New Mexico), and the Balcones Escarpment (Texas) likely have acted as intermittent physical barriers to gene flow among the distinct mitochondrial clades, which we recognize as subspecies within *C. hispidus*.

Key words: Heteromyidae, mitochondrial DNA, morphometrics, population genetics, systematics

DOI: 10.1644/11-MAMM-A-341.3

The hispid pocket mouse, *Chaetodipus hispidus* (Rodentia: Heteromyidae), is one of the most morphologically and genetically divergent species within the genus *Chaetodipus* (Hafner and Hafner 1983; Hafner et al. 2007; Hoffmeister 1986; Patton and Rogers 1993; Patton et al. 1981). Compared to other *Chaetodipus* species, *C. hispidus* is larger and possesses distinctive premolars, glans penes, bacula, and sperm (Paulson 1988). The 4 currently recognized subspecies of *C. hispidus* (*C. h. hispidus*, *C. h. paradoxus*, *C. h. spilotus*, and *C. h. zacatecae*) occupy a large geographic range extending from southwestern North Dakota (Geluso and Wright 2010) south through the Great Plains into Mexico (Fig. 1). *C. h. zacatecae* represents a disjunct distribution in central Mexico, ranging from southern Coahuila and Durango to Hidalgo (Fig. 1). The geographic distribution of the species ranges farther east and north (including colder continental zones of the northern Great Plains) than any other species in the genus.

Despite the many unique qualities of the hispid pocket mouse, there has been only 1 study exclusively focused on this heteromyid species. More than 60 years ago, Glass (1947) addressed morphological and geographic variation within *C. hispidus* in light of its long taxonomic history: since the original description in 1858, 7 different names have been proposed for populations of this species (e.g., Allen 1894; Elliot 1903; Merriam 1889; Osgood 1900). Glass (1947) examined 377 specimens and concluded that 4 subspecies should be recognized even though there was often extensive morphological intergradation among *C. h. hispidus*, *C. h. paradoxus*, and *C. h. spilotus* (*C. h. zacatecae* was not examined rigorously in his study due to a lack of material). This work, as well as early species and subspecies descriptions (e.g., Allen 1894; Elliot 1903; Merriam 1889; Osgood 1900), all indicate a lack of discrete morphological differences among subspecies.

The geographic distribution of the 3 subspecies evaluated by Glass (1947), as well as that of *C. h. zacatecae*, does not appear to coincide with obvious regional geographic features that may inhibit or intermittently block gene flow among subspecies of *C. hispidus*. For example, the Balcones Escarpment (a bundle of broken fault lines in central Texas [Fig. 1]) marks east–west

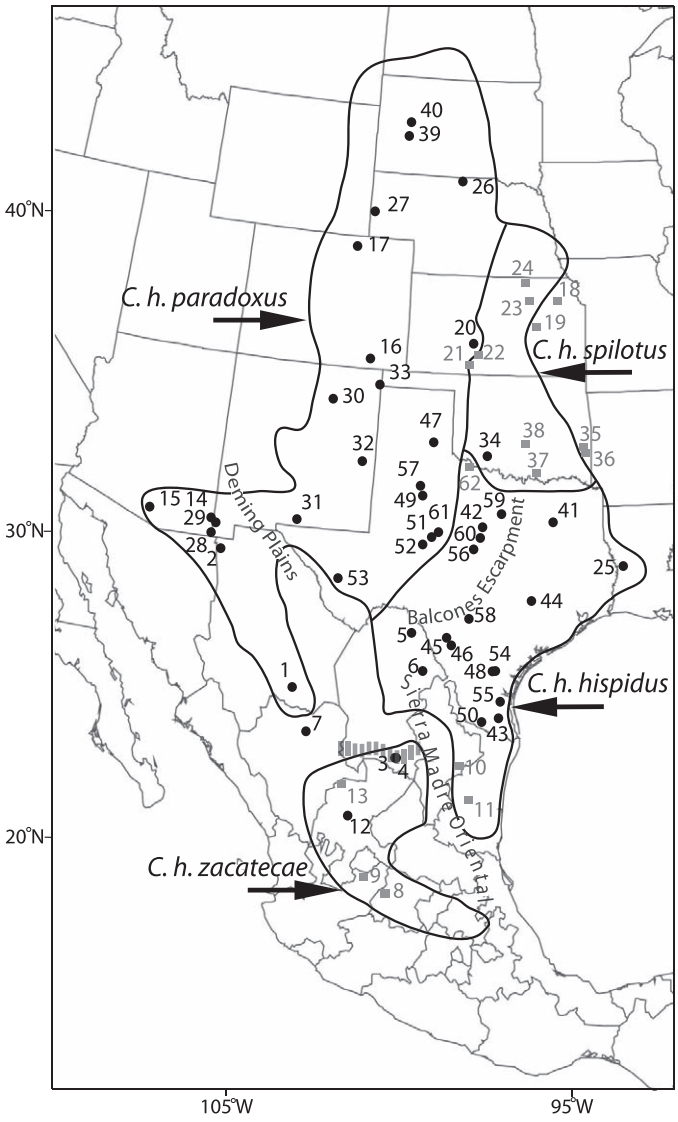

Fig. 1.—Geographic distribution of hispid pocket mouse (*Chaetodipus hispidus*) specimens used in the molecular phylogenetic analyses. Numbers refer to collecting localities listed in Appendix I and subspecies ranges based on Glass (1947), Hall (1981), and Hoffmeister (1986) are outlined in black. Fresh tissue and museum skin snip specimens are represented in black (filled circles) and in gray (filled squares), respectively.

shifts in the physical landscape, vegetation, and climate and has been shown to act as a dispersal barrier for several plant and animal taxa (Gehlbach 1991; Smith and Buechner 1947). Major rivers and associated riparian corridors such as the Río Grande also may serve as a potential barrier among populations (Amman and Bradley 2004). The Southern Coahuila filter-barrier (Baker 1956; Hafner et al. 2008) effectively divides the northern and southern altiplano of Mexico through a system of rivers and a terminal basin that were historically prone to severe flooding, as well as the western extension of the northernmost Sierra Madre Oriental. This terminal basin (The Laguna or Desierto Mayrán, depending on the season) likely persisted as one of the various Pleistocene pluvial lakes in the region. Of the 16 rodent species whose ranges occur in the general vicinity of the Southern Coahuila filter-barrier, 15 have species or subspecies boundaries that coincide with the filter-barrier (Hafner et al. 2008). Lastly, the Sierra Madre Oriental also may act to reduce east–west gene flow among altiplano and coastal populations of lowland species (Anducho-Reyes et al. 2008; Fa and Morales 1993; Guevara-Chumacero et al. 2010; McCormack et al. 2008; Riddle et al. 2000a).

Phylogeographic assessments allow researchers to identify evolutionarily unique units and to explain how past climatic cycles, geological changes, and anthropogenic effects may serve as potential barriers to gene flow within and among natural populations. Discovering these barriers could shed light upon the biogeographical history of a region and give a more robust understanding of past evolutionary processes. North America is a continent riddled with barriers that are known to limit gene flow within taxa (Jezkova et al. 2009; Kerhoulas and Arbogast 2010; McKnight 2005; Riddle 1995; Riddle and Hafner 2006; Riddle et al. 2000a). Whether these barriers cause genetic differences among subspecies or populations of *C. hispidus* is currently unknown. Herein, we use mitochondrial DNA (mtDNA) from both fresh tissue and museum specimens as well as morphological data from museum specimens to provide an assessment of phylogeographic variation within *C. hispidus*, and to assess the potential role of regional geographic features in effective genetic structure within the species.

Materials and Methods

Specimens examined.—Sixty-three specimens from 62 localities were examined in the mtDNA genetic analyses (16 of these specimens were obtained from museum study skins [Fig. 1 and Appendix I]) and 303 specimens from 254 localities were included in the morphological analyses (Appendix II). Outgroup taxa for genetic analyses were *C. baileyi* and *C. formosus*. These taxa were chosen as outgroups because *C. formosus* was identified as the sister taxon of *C. hispidus* by Hafner et al. (2007), and although the placement of *C. baileyi* is uncertain within the genus, it was hypothesized to be closely related to *C. formosus* by Alexander and Riddle (2005). Inclusion of an additional outgroup taxon (*C. californicus*; GenBank accession numbers AY009242 for the cytochrome-b gene [*Cytb*] and AY009259 for the cytochrome oxidase subunit III gene [COIII]) was not necessary as it did not result in any topological changes within the ingroup. All genetic samples were obtained as tissue loans from natural history museums (Appendix I).

Laboratory methods for fresh and museum skin snip tissues.—Mitochondrial DNA was extracted using the DNeasy Tissue Kit or the QIAamp DNA Mini Kit (QIAGEN Inc., Valencia, California) according to manufacturer's instructions; skin snips from museum study skins were presoaked in a 1X phosphate-buffered saline buffer solution for 24 h prior to extraction process. Extractions of fresh tissues were amplified by polymerase chain reaction for portions of the

mitochondrial genes COIII (672 base pairs [bp]), *Cytb* (417 bp), and reduced nicotinamide adenine dinucleotide dehydrogenase 2 (ND2; 969 bp) using the primers L8586 and H9323 (Riddle 1995), MVZ04 and MVZ05 (Smith and Patton 1991), and L5219ND2 and H6315ND2 (Sorenson et al. 1999), respectively. Extractions of skin snips from museum study skins were amplified for *Cytb* and ND2 using newly designed primers listed in Appendix III. Fragment lengths ranged from 163 to 369 bp for *Cytb* (average 247 bp) and 296 to 655 bp for ND2 (average 491 bp). Polymerase chain reactions for fresh tissues were performed in 25-µl reaction volumes using 10 µl of Eppendorf HotMaster PCR Mix (Fisher Scientific, Pittsburgh, PA), 1 µl of each primer (at 10 mM), and 1 µl of DNA template. Thermal-cycling parameters for COIII and *Cytb* required an initial denaturation at 94°C for 2 min, followed by 40 cycles of 94°C (60 s), 54°C (60 s), and 65°C (60 s), and a final extension of 65°C for 10 min. Thermal-cycling parameters for ND2 required an initial denaturation at 94°C for 5 min, followed by 30 cycles of 94°C (30 s), 50°C (30 s), and 65°C (90 s), and a final extension of 65°C for 5 min. Polymerase chain reactions for skin snips from museum study skins were performed in 25-µl reaction volumes using 4 µl of $MgCl_2$, 2.5 µl of 10X buffer, 2 µl of deoxynucleoside triphosphate, 2 µl of 5 M betaine, 1 µl of each primer (at 10 mM), and 0.125 µl of rTaq DNA Polymerase (TaKaRa, Mountain View, CA). Thermal-cycling parameters required an initial denaturation at 94°C for 2 min, followed by 40 cycles of 94°C (30 s), 48–53°C (30 s), and 72°C (30 s), and a final extension of 72°C for 5 min. All amplified products were purified using EXOSap-IT (USB Corporation, Cleveland, OH) and all sequencing reactions were performed at the University of Florida DNA Sequencing Core Laboratory (Gainesville, Florida) using ABI Prism BigDye Terminator cycle sequencing protocols (Applied Biosystems, Foster City, CA) as described in Light and Reed (2009). Sequences were edited using Sequencher 4.9 (GeneCodes Corporation, Madison, WI), and primer sequences were removed and sequences trimmed in reference to the translated protein sequence using Se-Al version 2.01a11 (Rambaut 1996). Sequences were aligned by eye using Se-Al version 2.01a11 (Rambaut 1996) and all sequences were submitted to GenBank (GenBank accession numbers JQ412006–JQ412054 for COIII, JQ411942–JQ412005 for *Cytb*, and JQ411873–JQ411941 for ND2).

Phylogenetic analysis.—Rigorous phylogenetic analyses were performed on 3 main data sets. The 1st data set included only fresh tissue samples consisting of 47 ingroup taxa and the mitochondrial genes were analyzed individually as well as in a combined 3-gene framework. The 2nd and 3rd data sets included both fresh tissue samples and museum skin snips. Unfortunately, not all of the small gene fragments of *Cytb* and ND2 (Appendix III) amplified and sequenced. To avoid having excessive amounts of missing data in our analyses, museum skin snip samples were analyzed only if we were able to successfully amplify and sequence a combined total of at least 3 fragments from *Cytb* or ND2, or both. The data sets including both fresh tissue samples and museum skin snips had a total of 63 ingroup taxa and consisted of either 2 genes (*Cytb* and ND2) or 3 genes (COIII, *Cytb*, and ND2; all skin snip samples were missing COIII data). As with the fresh tissue–only data set, mitochondrial genes in the 63-taxon data sets were analyzed individually as well as in a combined 2-gene or 3-gene framework. Phylogenetic analyses were conducted on all data sets using neighbor-joining, maximum-parsimony, maximum-likelihood, and Bayesian approaches in PAUP* version 4.0b10 (Swofford 2003); Randomized Axelerated Maximum-Likelihood (RAxML—Stamatakis 2006); and MrBayes version 3.1.2 (Ronquist and Huelsenbeck 2003). Distance-based neighbor-joining analyses and equally weighted maximum-parsimony heuristic searches with 10 random addition replicates and tree-bisection-reconnection branch swapping were performed using PAUP* version 4.0b10 (Swofford 2003). Support for these nodes was tested with 200 nonparametric bootstrap replicates (10 random sequence additions—Felsenstein 1985).

Best-fit models of nucleotide substitution for the maximum-likelihood analyses were selected using the Akaike information criterion (Huelsenbeck and Rannala 1997; Posada and Buckley 2004) in the program ModelTest (version 3.6—Posada and Crandall 1998). Best-fit models of evolution are listed in Appendix IV. Full heuristic maximum-likelihood and bootstrap searches (1,000 pseudoreplicates) were conducted using the preferred models in RAxML (Stamatakis 2006).

Bayesian phylogenetic analyses were performed in partitioned and nonpartitioned frameworks. Genes were partitioned by gene, codon position (each codon position separately as well as linking the 1st and 2nd positions with the 3rd position treated as an independent partition), and by gene and codon position (again, each codon position separately as well as linking the 1st and 2nd positions with the 3rd position treated as an independent partition). Best-fit models of evolution were determined using MrModeltest (version 2.3—Nylander et al. 2004) and are listed in Appendix IV. To choose the best partitioning scheme, Bayes factors were computed using the harmonic means of the likelihoods calculated from the *sump* command within MrBayes. A difference of 2 ln Bayes factor $>$ 10 was used as the minimum value to discriminate between analysis schemes (Bradley et al. 2004; Brown and Lemmon 2007). For the 47-taxon fresh tissue samples–only data set, partitioning by gene and codon position (with each codon position treated as a separate partition) was identified as the best fit to the data. For the 63-taxon data sets including both fresh tissue samples and museum skin snips, partitioning by codon position but linking the 1st and 2nd positions was selected as the best-fit model for the 2-gene data set, whereas partitioning only by codon position (with each codon position treated as a separate partition) was selected as the best model for the 3-gene data set.

In the Bayesian phylogenetic analyses, model parameters were treated as unknown variables with uniform priors, and in the partitioned analyses all partitions were unlinked. Bayesian analyses were initiated with random starting trees, run for 10 million generations with 4 incrementally heated chains

(Metropolis-coupled Markov chain Monte Carlo—Huelsenbeck and Ronquist 2001), and sampled at intervals of 1,000 generations. Stationarity was assessed and all burn-in points (2,000 trees) were discarded. The retained equilibrium samples were used to generate a 50% majority-rule consensus tree with the percentage of samples recovering any particular clade representing that clade's posterior probability (Huelsenbeck and Ronquist 2001).

Estimates of divergence times.—We used the program BEAST version 1.6.1 (Drummond et al. 2006; Drummond and Rambaut 2007) and the 47-taxon data set to estimate divergence times within *C. hispidus*. Although there is no known fossil for *C. hispidus*, Hafner et al. (2007) estimated the mean divergence between *C. formosus* and *C. hispidus* to be 13.07 million years ago (mya) with a 95% highest posterior density interval (95% HPD) of 10.41–15.74 mya. We employed a normal distribution for this mean prior and assigned a standard deviation of 1 for the split between *C. formosus* and *C. hispidus* on the 3-gene 47-taxon data set (in a nonpartitioned and partitioned framework). We recognize that use of a secondary calibration point is not ideal in divergence-dating analyses and could potentially result in incorrect estimates of divergence times. However, this calibration is the only option at this time. Preliminary BEAST analyses resulted in the parameter ucld.stdev (the standard deviation of the uncorrelated lognormal relaxed clock) being significantly different from 0, which indicates that the data for *C. hispidus* are not clocklike. Therefore we enforced a relaxed, uncorrelated lognormal clock for our substitution rate. In BEAST, a Yule process speciation prior and an uncorrelated lognormal model of rate variation were implemented in each analysis. The best-fit model of nucleotide substitution for the nonpartitioned and partitioned 3-gene data sets was selected as determined above. Two separate Markov chain Monte Carlo analyses were run for 30,000,000 generations with parameters sampled every 1,000 steps, and a 10% burn-in. Independent runs were combined using LogCombiner version 1.6.1 (Drummond and Rambaut 2007). TRACER version 1.5 (Rambaut and Drummond 2004) was used to measure the effective sample size of each parameter (all resulting effective sample sizes exceeded 200) and calculate the mean and upper and lower bounds of the 95% HPD for divergence times. Tree topologies were assessed using TreeAnnotator version 1.6.1 (Drummond and Rambaut 2007) and FigTree version 1.3.1 (Rambaut 2008).

Network and population genetic analyses.—If the specimens examined in this study are recently diverged with only a small number of substitutions differentiating haplotypes, then interspecific methodologies such as phylogenetic analyses may mask evolutionary processes within hispid pocket mice. Rather, intraspecific methodologies such as network and population genetic analyses may be preferred to reveal processes such as gene flow and thus gain a better understanding of species history (Cassens et al. 2003; Crandall 1996; Crandall and Templeton 1996; Demboski and Sullivan 2003). Therefore, in addition to our phylogenetic analyses of *C. hispidus*, we also examined the mitochondrial data using network and population genetic analyses.

Only sequences from fresh tissue samples (47-taxon data set) were used for network and population genetic analyses because of large amounts of missing data in the sequences from museum skin snip specimens. Haplotype networks were constructed for each gene and the combined 3-gene data set. A statistical parsimony analysis (Templeton et al. 1992) using TCS 1.21 software (Clement et al. 2000) was performed to assemble the most-parsimonious haplotype tree (with linkages between taxa representing mutational events) and estimate a 95% plausible set for all haplotype connections.

The computer programs Arlequin version 3.5 (Excoffier et al. 2005) and DnaSP (version 5.1—Rozas et al. 2003) were used to calculate population genetic statistics including haplotype diversity (h), nucleotide diversity (π), uncorrected genetic distances, F_{ST} statistics, and Tajima's D-test of selective neutrality (Tajima 1989). Population structure and population pairwise ϕ_{ST} values were assessed with an analysis of molecular variance (AMOVA—Excoffier et al. 1992). In these analyses, populations were defined a priori by subspecies and mitochondrial clade (as determined in the phylogenetic analyses) and significance was assessed by 10,000 randomization replicates. Arlequin also was used to calculate Fu's F-statistics (Fu 1997) and mismatch distributions to examine the demographic history of *C. hispidus*.

We used the program SAMOVA 1.0 (Dupanloup et al. 2002) to conduct a spatial analysis of molecular variance (SAMOVA) in an attempt to detect genetic barriers among inferred populations. This program identifies groups of populations (K) that are maximally differentiated from each other (F_{CT} index) without defining populations a priori. Each locality was considered a population and analyses were run for 10,000 iterations and 100 initial conditions for $K = 1, 2, 3, \ldots,$ 10 groups. To assess correlation between population pairwise genetic distance and geographical distance, Mantel tests were performed using the program Alleles In Space (AIS—Miller 2005).

Morphological analysis.—Specimens examined morphologically included the holotypes and topotypes of 3 of the 4 subspecies of *C. hispidus* (excluding *C. h. spilotus* [Appendix II]). A total of 303 specimens (129 females and 174 males) were used in the morphological analyses and there was little specimen overlap between the morphological and molecular aspects of this study (Appendix I and Appendix II). All specimens were adults with closed cranial sutures and occipital–nasal lengths (ONLs) greater than 25 mm. Eleven cranial characters were measured, including ONL, occipital–incisor length (OIL), nasal length (NL), rostral width (RW), width of interorbital constriction (IOC), zygomatic breadth (ZB), cranial width (CW), mastoid breadth (MB), diastema length (DIA), occlusal length of the upper premolar (LPM), and occlusal length of the upper molars (LM). Univariate and multivariate statistical analyses were performed using SYSTAT 8.0 (SPSS Inc. 1996). The measured cranial characters for specimens of *C. hispidus* were examined for

sexual dimorphism using an unpaired *t*-test. Past work has not shown strong sexual dimorphism in *Chaetodipus* (Best 1993; Glass 1947), and our results support this finding ($P > 0.05$ for all characters except for IOC without a Bonferroni adjustment). Accordingly, males and females were analyzed together.

To decrease the effect of individual size variation, all characters were transformed logarithmically and standardized (Burbrink 2001; Corruccini 1975; dos Reis et al. 1990; Gould 1966). Discriminant function analyses were performed on both the raw and size-adjusted characters to determine if hispid pocket mice could be separated with a priori hypotheses of group membership to subspecies and to the mitochondrial clades identified in this study. The analyses generated classification matrices (jackknifed and unjackknifed) that showed the percentage of specimens correctly assigned to their a priori groupings.

Results

Phylogenetic analysis.—All analyses recovered *C. hispidus* as a monophyletic group. Phylogenetic analyses of individual genes and the combined 3-gene data set (2,049 bp) of fresh tissue samples (47-taxon data set) resulted in no topological conflict regardless of the phylogenetic method used. The results of the Bayesian and maximum-likelihood analyses of the combined 3-gene data set are presented in Fig. 2 and results from all other analyses are available upon request. Although our sample of the subspecies *C. h. spilotus* ($n = 1$) was not large enough to address the issue of subspecies monophyly, the subspecies *C. h. hispidus*, *C. h. paradoxus*, and *C. h. zacatecae* are not reciprocally monophyletic based on these data (Fig. 2). Rather, phylogenetic analyses divide *C. hispidus* into 4 mitochondrial clades (clades A–D; Fig. 2), two of which are composed of mixtures of assigned subspecies. Clades B and C received strong support in all analyses (Fig. 2). Although support for clade D and the node uniting clades B, C, and D was low in Fig. 2 (Bayesian posterior probability = 0.81 and 0.82, respectively), posterior probabilities were always greater than 0.98 in all other Bayesian analyses (Fig. 2 and data available upon request). Support for clade A was weak (Fig. 2 and other Bayesian analyses), however there usually was strong to moderate support uniting clades B, C, and D (see above) apart from clade A.

For the combined 3-gene data set, genetic divergences within each clade were small, ranging from 0.1% to 1.1% (uncorrected *p*-distances), with highest divergence observed within clade D. Higher genetic divergence was observed among clades ranging between 2.4% and 3.9%, with clade A being the most divergent group (3.9%, 3.8%, and 3.5% to clades B, C, and D, respectively). Of the 3 mitochondrial genes examined in this study, ND2 was the most variable, with genetic divergences ranging from 2.8% to 4.7% among clades. Examination of the ND2 data also shows that clade A is the most divergent group (4.7%, 4.5%, and 4.0% divergence from clades B, C, and D, respectively).

Monophyly of the 4 subspecies of *C. hispidus* also was assessed when museum skin snip samples were included in the analyses, resulting in larger sample sizes of both *C. h. spilotus* ($n = 11$) and *C. h. zacatecae* ($n = 7$). The results of the Bayesian and maximum-likelihood analyses of the 63-taxon data set for the combined 3-gene data set are presented in Fig. 3. Results of the 2-gene and 3-gene data sets were similar, although support values were larger in the 3-gene data set (results available upon request). Notably, analyses of this 3-gene data set further supported 4 mitochondrial clades (clades A–D; Fig. 3) and lack of monophyly of all 4 subspecies. Even in the presence of substantial missing data from the COIII gene, support values when fresh tissue and museum skin snip samples were analyzed together were similar to those when only fresh tissues were examined. Clades B and C continue to receive strong support in the Bayesian analysis (Bayesian posterior probability ≥ 0.99), and clade C also is well supported in the maximum likelihood analysis (bootstrap support = 92). Genetic divergences within and among clades were nearly identical to those of the 3-gene data set using only fresh tissue samples (results available upon request).

Estimates of divergence times.—Divergence-dating analyses for the 3-gene nonpartitioned data set estimated the origin of *C. hispidus* to be 7.39 mya (3.61–11.25 mya 95% HPD). Clades B, C, and D last shared a common ancestor 5.37 mya (2.52–8.68 mya 95% HPD). Lineage divergence within clades A, B, C, and D all occurred within the last 4 mya: 0.70 mya (0.005–2.13 mya 95% HPD), 2.49 mya (0.73–4.68 mya 95% HPD), 2.65 mya (0.88–4.79 mya 95% HPD), and 3.89 mya (1.61–6.57 mya 95% HPD), respectively. Divergence estimates were slightly younger in the partitioned data set (data available upon request).

Network and population genetic analyses.—Network analyses of the combined 3-gene data set resulted in 6 unconnected subnetworks corresponding to clades A and B, 2 subnetworks of clade C where 1 subnetwork consists solely of the most southern sample in Zacatecas, Mexico (CIB 16674; locality 12), and a northern and southern subnetwork of clade D (Appendix I; all networks are available upon request). When the connection limit was lowered to 90%, 4 unconnected subnetworks were resolved corresponding to the 4 mitochondrial clades. The clade D subnetwork showed a fair amount of reticulation (results available upon request) and network analyses of individual genes always resulted in an unconnected subnetwork corresponding to clade A and representatives from clades B, C, and D either formed separate subnetworks (ND2) or 1 large subnetwork (COIII and *Cytb*).

For the remaining population genetic studies, it is important to note that our sample size was small. We sampled a total of 47 individuals and, in all cases except 1, there was 1 individual per population (Appendix I). However, when mitochondrial clades were treated as populations (as they were for the majority of the population genetic analyses), sample sizes were larger, with 3, 7, 11, and 26 specimens for clades A, B, C, and D, respectively. Still, the results of the population genetic

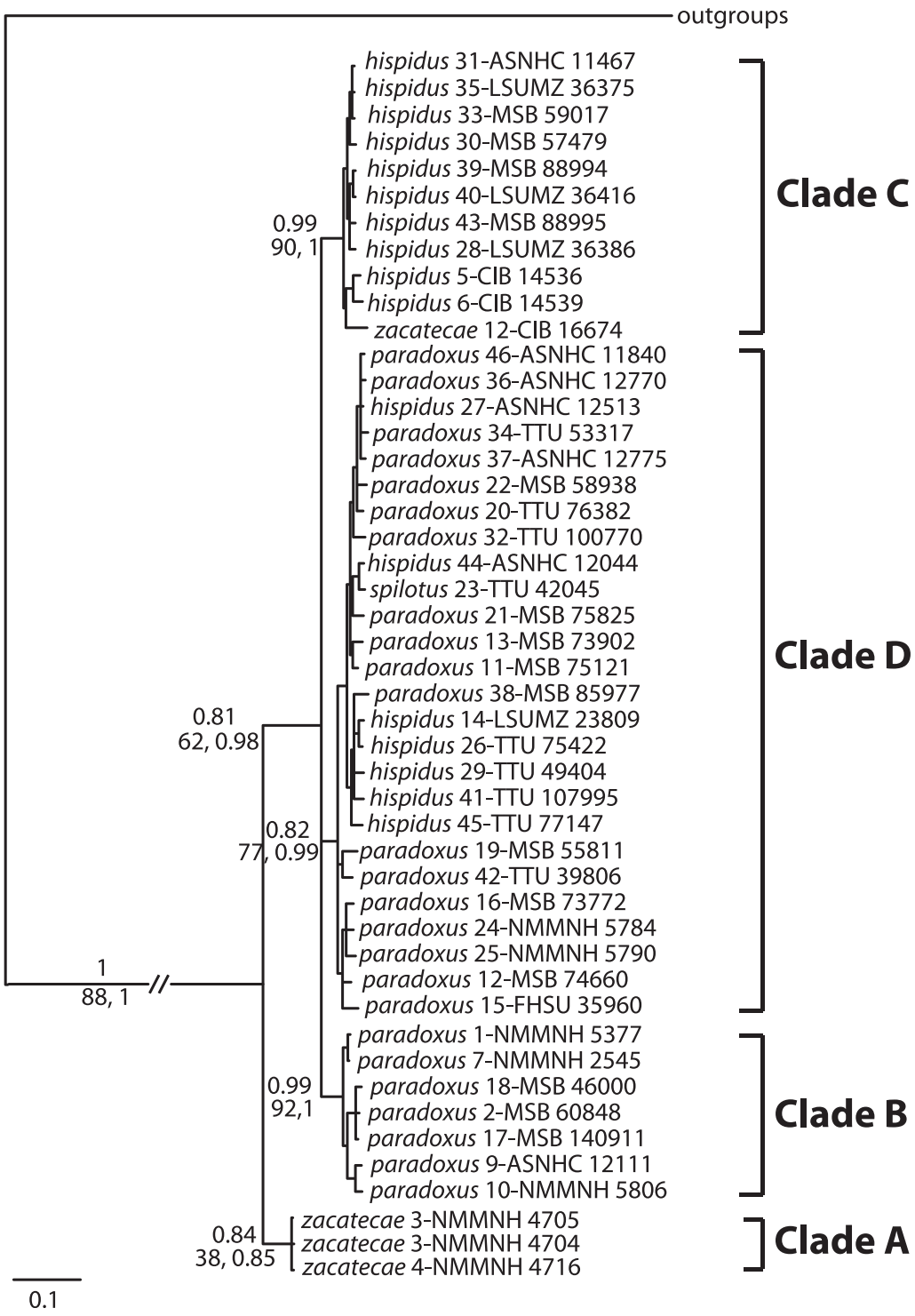

Fig. 2.—Bayesian phylogram resulting from a partitioned analysis (by gene and codon position) of the cytochrome oxidase subunit III (COIII), cytochrome *b* (*Cytb*), and reduced nicotinamide adenine dinucleotide dehydrogenase 2 (ND2) genes for 47 specimens of *Chaetodipus hispidus* for which there were fresh tissues available (specimens without asterisks [*] in Appendix I). At nodes of interest, Bayesian posterior probability values from the partitioned analysis are indicated above the nodes, and maximum-likelihood bootstrap support values and Bayesian posterior probability values from the nonpartitioned analysis are indicated below the nodes, respectively. Support values at terminal nodes are available upon request. Taxa are listed by traditional subspecies name followed by locality number and museum specimen number (Fig. 1 and Appendix I). Mitochondrial clades are indicated to the right of the phylogeny.

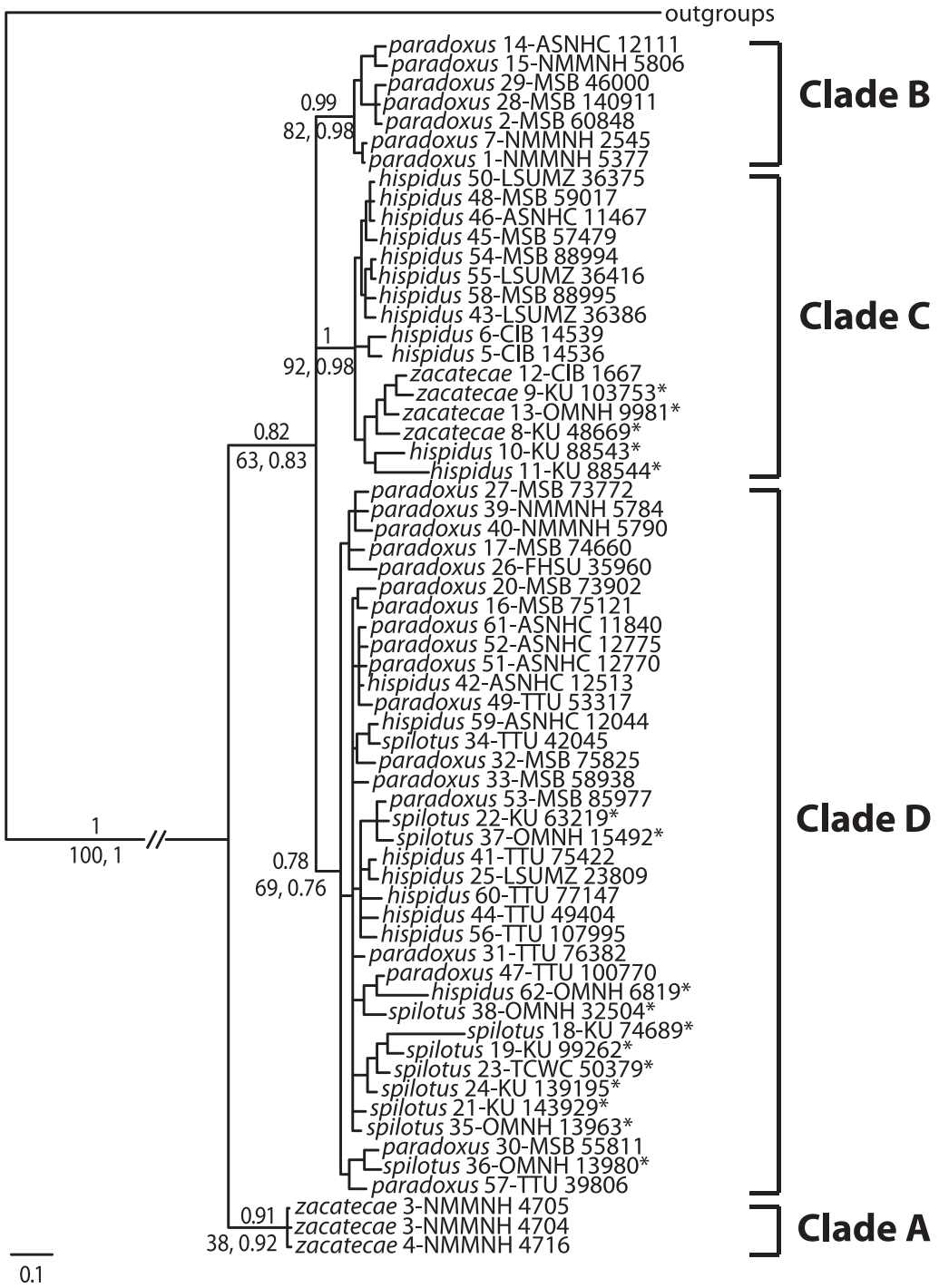

Fig. 3.—Bayesian phylogram resulting from partitioned analysis (by codon) of the cytochrome oxidase subunit III (COIII), cytochrome *b* (*Cytb*), and reduced nicotinamide adenine dinucleotide dehydrogenase 2 (ND2) genes for 63 specimens of *Chaetodipus hispidus* (all specimens for which there were fresh and museum skin snip tissues available [Appendix I]). At nodes of interest, Bayesian posterior probability values from the partitioned analysis are indicated above the nodes, and maximum-likelihood bootstrap support values and Bayesian posterior probability values from the nonpartitioned analysis are indicated below the nodes, respectively. Support values at terminal nodes are available upon request. Taxa are listed by traditional subspecies name followed by locality number and museum specimen number (Fig. 1 and Appendix I). Museum specimens for which skin snips were used to collect genetic data are indicated with asterisks (*). Mitochondrial clades are indicated to the right of the phylogeny.

TABLE 1.—Population genetic statistics for the combined 3-gene data set of the hispid pocket mouse (*Chaetodipus hispidus*) for all populations and the mitochondrial clades determined in phylogenetic analyses (clades A, B, C, and D; Fig. 2). Statistics include sample size (n), haplotype diversity (h), nucleotide diversity (π), Tajimas's D, Fu's F_S, and mismatch distribution parameters for the sudden expansion model (shape of the mismatch distribution; population size before expansion [θ_0]; population size after expansion [θ_1]; expansion parameter [τ]; Harpending's raggedness index [Ragged]). Mismatch distribution graphs are available upon request. Note that the sample size for clade A was small ($n = 3$) and results of this clade should be interpreted with caution. Results were similar when mitochondrial genes were analyzed independently. Asterisks (*) indicate statistically significant values ($P < 0.05$).

	n	h	π	Tajima's D	Fu's F	Mismatch	θ_0	θ_1	τ	Ragged
All	47	1	0.01989	−1.26175	−19.90834*	Multimodal	42.887	418.525	13.75	0.0017
Clade A	3	1	0.00065	—	—	Unimodal	0	99999	1.629	0.6667
Clade B	7	1	0.00671	−0.0281	−1.0173	Multimodal	0	126.797	17.217	0.0317
Clade C	11	1	0.00653	−1.53730	−3.288*	Multimodal	10.322	737.6	4.934	0.06942
Clade D	26	1	0.01015	−1.956*	−11.5073*	Multimodal	3.987	225.513	19.131	0.0049

analyses should be interpreted cautiously and more extensive sampling will be necessary for future studies wishing to fully evaluate population processes within *C. hispidus*.

Every sequence of the combined 3-gene data set was unique (i.e., high haplotype diversity) and nucleotide diversity was low, indicating that most haplotypes were closely related and that *C. hispidus* may have undergone a recent population expansion (Table 1). Fu's neutrality test also supports a recent population expansion (a significantly negative F-statistic indicates rapid population expansion), but only for the entire sample and clades C and D. Similarly, results of Tajima's D neutrality tests were negative (also indicating population expansion), but only significantly so for clade D. The shape of the mismatch distribution (unimodal, bimodal, or multimodal) indicates a population expansion (unimodal distribution—Rogers and Harpending 1992) or a relatively stable demographic history (bi- or multimodal distribution—Ray et al. 2003). In apparent conflict with the other population analyses, the mismatch distribution analysis for the entire sample and clades B, C, and D was multimodal (graphs available upon request), suggesting stable demographic histories for each clade (Ray et al. 2003; Table 2). However, the null hypothesis of population expansion cannot be rejected with a nonsignificant raggedness index (Ragged; Table 1). The small sample size of clade A precludes a clear understanding of the population history of this lineage.

Analysis of molecular variation of the combined 3-gene data set revealed significant population structuring, with 69.02% of the variation distributed among the mitochondrial clades (pairwise $\phi_{CT} = 0.690$; Table 2). Results were substantially different when AMOVA was performed on the 4 subspecies where a majority of the variation was distributed within each subspecies (pairwise $\phi_{CT} = 0.295$; Table 2). Pairwise estimates of mitochondrial DNA F_{ST} for mitochondrial clades calculated in DnaSP ranged from 0.650 (clades B and D) to 0.906 (clades A and C), with all F_{ST} values greater than 0.851 between clade A and clades B, C, and D. These results indicate there likely is some, albeit limited, gene flow among the mitochondrial clades.

Although we had only 1 sample per population (locality), the results from SAMOVA support the findings from the phylogenetic, network, and other population analyses (see above), finding that the best partitioning scheme of genetic diversity was obtained with $K = 4$ corresponding to clades A–D. For the combined 3-gene and ND2 data sets, F_{CT} values at $K = 4$ were high (0.69 and 0.735, respectively) and statistically significant ($P < 0.05$). Increasing values of K resulted in minimal increases of F_{CT} values and further subdivision within clades B, C, or D. For the COIII and *Cytb* data sets, all F_{SC} and F_{ST} values were 1, with high and statistically significant F_{CT} values at $K = 6$ (0.735 and 0.646, respectively; F_{CT} values increased minimally with increasing K). These 6 groups correspond to the 4 mitochondrial clades and subdivision with

TABLE 2.—Analysis of molecular variance for the 4 subspecies (*Chaetodipus hispidus hispidus*, *C. h. paraxodus*, *C. h. spilotus*, and *C. h. zacatecae*) and the 4 mitochondrial clades (clades A, B, C, and D; Fig. 2) of the hispid pocket mouse, indicating the degree and significance of population structuring for the combined 3-gene data set.[a] Significance of variance component (P) is indicated with an asterisk (*) and was tested by permutation according to Excoffier et al. (1992).

Source of variation	*d.f.*	Variance components	Sum of squares	Percentage of variation	Fixation indexes
Chaetodipus hispidus subspecies					
Among groups	3	6.845	242.406	29.51	$\phi_{CT} = 0.295$*
Among populations within subspecies	42	15.847	694.477	68.33	$\phi_{SC} = 0.969$
Within populations	1	0.5	0.5	2.16	$\phi_{ST} = 0.978$*
Chaetodipus hispidus mitochondrial clades					
Among groups	3	18.960	575.750	69.02	$\phi_{CT} = 0.690$*
Among populations within clades	42	8.011	360.133	29.16	$\phi_{SC} = 0.941$
Within populations	1	0.5	0.5	1.82	$\phi_{ST} = 0.982$*

[a] Results were similar for each gene analyzed individually.

clades C and D (COIII data set) or clades B and C with combination of some localities from both of these clades (*Cytb* data set). In general, we found that subdivisions greater than $K = 4$ did not produce additional informative clusters. Mantel tests detected significant correlation between geographical distance and pairwise genetic distance values when all samples were grouped together ($r = 0.2225$; $P < 0.05$), in clade B ($r = 0.41026$; $P < 0.05$), and in clade C ($r = 0.709103$; $P < 0.005$). There was no isolation by distance detected within clades A and D ($P > 0.05$).

Morphological analysis.—The 303 specimens analyzed morphologically belonged to clades B ($n = 20$), C ($n = 80$), and D ($n = 203$; no specimens could be assigned to clade A) and represented the subspecies *C. h. hispidus* ($n = 75$), *C. h. paradoxus* ($n = 128$), *C. h. spilotus* ($n = 75$), and *C. h. zacatecae* ($n = 25$; Appendix II). Discriminant function analysis was not able to consistently discriminate among either the 4 clades (Fig. 4A) or the 4 subspecies (Fig. 4B) of *C. hispidus* using the cranial characters selected for analysis. Results for the different data treatments (standardized and log transformed) were similar, with the log-transformed data presented below. A posteriori rates of correct classification into the 4 mitochondrial clades were 75% (clade B), 56% (clade C), and 76% (clade D) and a total of 88 (of 303) pocket mice were misclassified. Characters that showed high loading on the 1st discriminant function axis included ONL, ZB, CW, MB, DIA, and IOC. Characters with high loading on the 2nd discriminant function axis included ONL, MB, IOC, OIL, and CW. When specimens were analyzed by subspecies, a posteriori rates of correct classification were 71% (*C. h. hispidus*), 50% (*C. h. paradoxus*), 49% (*C. h. spilotus*), and 80% (*C. h. zacatecae*) and 129 pocket mice were misclassified. ONL, MB, IOC, and CW loaded heavily on the 1st discriminant function axis and IOC, CW, MB, and DIA loaded heavily on the 2nd discriminant function axis.

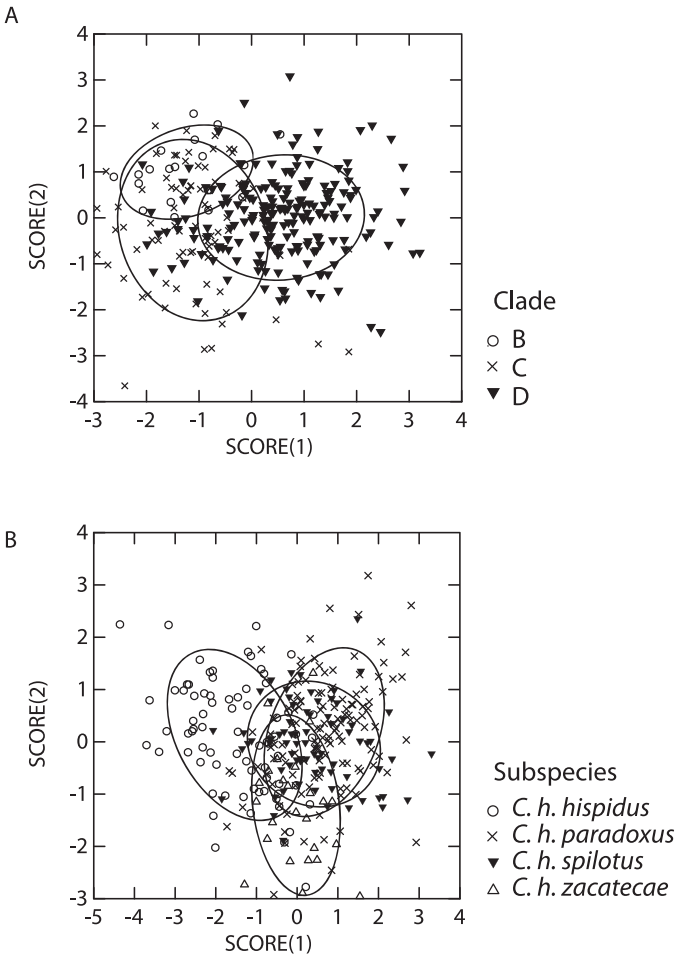

FIG. 4.—Discriminant function plot of standardized cranial measurements for 303 specimens of *Chaetodipus hispidus* belonging to A) 3 mitochondrial clades, clades B, C, and D, and B) the 4 subspecies, *C. h. hispidus*, *C. h. paradoxus*, *C. h. spilotus*, and *C. h. zacatecae*. The ovals surrounding each clade represent 95% confidence intervals.

DISCUSSION

This study demonstrates that the 4 currently recognized subspecies of *C. hispidus* are not genetically or morphologically distinct. Instead, we find 4 distinct mitochondrial clades of *C. hispidus* that do not correspond to currently recognized subspecies, but each of which is separated by ecological and geographical barriers (Fig. 5). The hispid pocket mouse is an arid grassland specialist (Paulson [1988] and references therein). Climatic (e.g., historical drying cycles intermittently interrupting and reconnecting continuous ranges) or possibly even recent historical anthropogenic (e.g., habitat loss due to agriculture) changes, or both, may have caused repeated expansion and contraction of the species' geographic range as it tracked suitable grassland habitat. These expansions and contractions, especially those in the Pliocene and Pleistocene, may have restricted genetic exchange within *C. hispidus*, possibly resulting in isolation of populations corresponding to our 4 mitochondrial clades. Although our population genetic analyses do indicate that gene flow is likely still occurring among some clades (Table 2), a larger sample size will be necessary to fully address population-level processes within *C. hispidus*.

Potential geological barriers affecting gene flow among the 4 mitochondrial clades include the Southern Coahuila filter-barrier, which divides the Chihuahuan Desert into 2 major subregions differing in topography and climate (Altiplano Norte and Altiplano Sur—Arriaga et al. 1997; Morrone 2005). The Southern Coahuila filter-barrier is located in the Chihuahuan Desert and is made up of 3 segments: a western extension of the Sierra Madre Oriental, the Ríos Nazas and Aguanaval, and the central Mayrán Basin. The Mayrán Basin is a terminal basin that is prone to flooding from the 2 rivers, particularly prior to recent installation of flood-control dams along the Río Nazas (Hafner et al. 2008). It is possible that large bodies of water persisted during pluvial periods in the Pleistocene (and possibly earlier), which may have caused the isolation of *C. hispidus* in north-central Mexico that is now represented by a remnant population corresponding to clade A

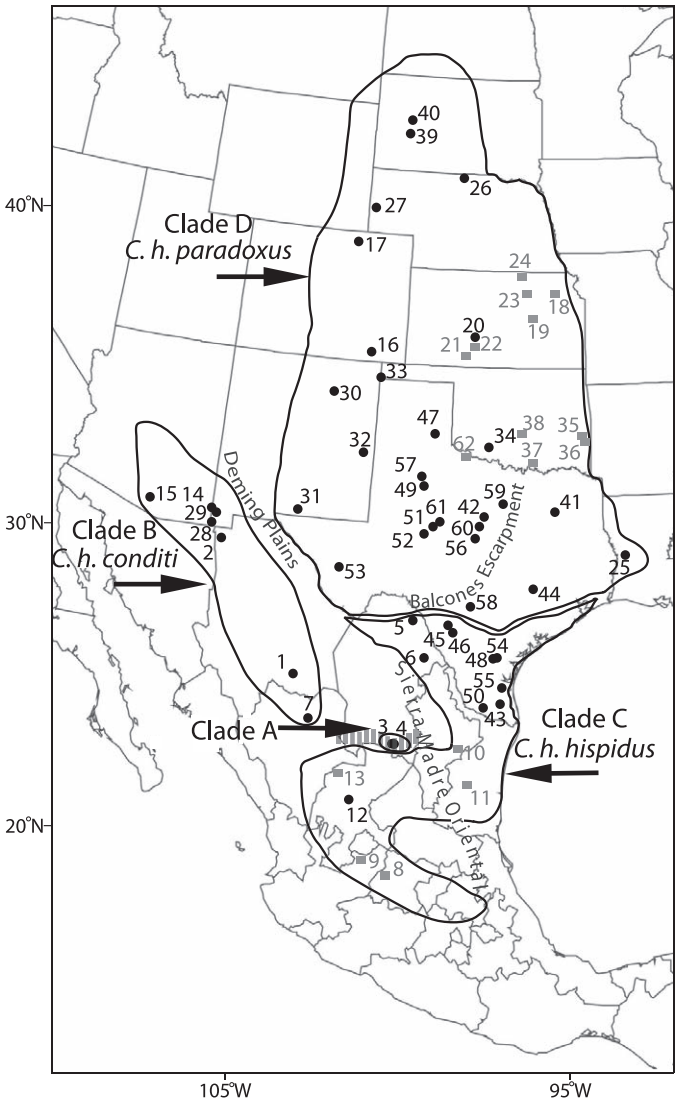

Fig. 5.—Geographic distribution of mitochondrial clades of *Chaetodipus hispidus* resulting from phylogenetic analyses. The Southern Coahuila filter-barrier is indicated by the stitched line. Numbers refer to collecting localities listed in Appendix I. Fresh tissue and museum skin snip specimens are represented in black (filled circles) and in gray (filled squares), respectively. Ranges of mitochondrial clades are outlined in black and encompass all genetic and morphological samples analyzed in this study (Figs. 1 and 2) as well as museum specimens available in MaNIS (http://manisnet.org). New subspecies names are indicated next to their respective clade.

(Fig. 5). During these pluvial periods, populations north and south of the Southern Coahuila filter-barrier probably adapted to their respective subregions and began to diverge from one another.

Along with the Southern Coahuila filter-barrier, the Sierra Madre Oriental may have served as a geological barrier between the subspecies *C. h. hispidus* and *C. h. zacatecae* (Fig. 1). This mountain range has been implicated as a barrier to gene flow in other mammal species with similar ranges (Guevara-Chumacero et al. 2010; Neiswenter and Riddle 2010.). The uplift of the Sierra Madre Oriental occurred during the early Eocene, which would have allowed for sufficient time to pass for separate, genetically isolated populations of mammals to form (Hafner and Riddle 2011). However, the Sierra Madre Oriental does not appear to serve as a barrier between *C. h. hispidus* and *C. h. zacatecae*. Rather, gene flow is ongoing between populations in northeastern Mexico and central and southern Mexico, likely through the central region of the Sierra Madre Oriental (clade C; Fig. 5). Therefore, although the Sierra Madre Oriental may be a barrier to gene flow in some mammals, it is not for *C. hispidus*. The large number of basins located within the mid–Sierra Madre Oriental (Dicken 1936) were formed by erosion and other geological processes (Schmidly 1974) and may provide suitable dispersal routes for several mammal species (Ceballos et al. 2010), especially for low grassland specialists such as *C. hispidus*.

In the western United States, climatic oscillations during mesic times may have temporarily restricted desert dwelling species on either side of the Deming Plains (Castoe et al. 2007). The Deming Plains, also known as the Cochise filter-barrier (Morafka 1977), is located along the continental divide between southwestern New Mexico and the Río Grande and creates an east–west boundary between the Sonoran and Chihuahuan deserts (Fig. 5; Hunt 1983). When warmer and drier interglacial periods occurred, the east–west boundary would disappear, desert brush would replace grasslands, and many taxa would be rejoined (Hafner and Riddle 2005; Riddle 1995). During cooler, more mesic times, the boundary would reappear, primarily represented by grassland habitat, reuniting grassland specialists such as *C. hispidus*. These periodic fragmentations may have caused divergence between clades B and D (Fig. 5). Similarly, climatic oscillations in southeastern Texas during the late Pliocene–Pleistocene resulted in repeated Gulf Coastal marine incursions (Riddle 1995; Riddle and Honeycutt 1990), which may have resulted in divergence and subsequent expansions of clades C and D (Fig. 5). Similar vicariant events have occurred in other taxa such as *Peromyscus attwateri* (Lack et al. 2010). As in our study, genetic diversity among populations of *P. attwateri* was generally low, indicating that not enough time has passed for populations to diverge substantially. Last, the Balcones Escarpment in Texas also may have played a role in shaping phylogeographic patterns between clades C and D in the western United States. A study of the herpetofauna of Texas found that a high percentage of species had geographic margins coincident with the Balcones Escarpment (Smith and Buechner 1947). It is probable that a combination of climatic shifts along the Balcones Escarpment resulted in divergence of clades C and D (Fig. 5).

Hafner et al. (2007) hypothesized that *C. hispidus* diverged from *C. formosus* in the mid-Miocene, approximately 13 mya. It is reasonable to assume that this divergence took place in central Mexico for several reasons: fossil evidence suggests that species distributions within the Heteromyidae never extended north of the United States–Mexico border until after the mid-Miocene (Wahlert 1993); the current range of *C. formosus* includes the southwestern United States and the Baja

Peninsula, which did not form until roughly 6 mya (Riddle et al. 2000b), suggesting that *C. formosus* was restricted to central and northern Mexico until it was able to expand its range after the Miocene; and clade A, restricted to north-central Mexico, is the most basal group in all phylogenetic analyses. Our divergence-dating analyses support the timing of these events (although we note that our estimates are based on a secondary calibration point and will require verification should more fossil evidence become available). Diversification within *C. hispidus* did not occur until ~7 mya and diversification within each clade was even more recent. It was not until the glacial–interglacial climatic oscillations of the Pliocene and Pleistocene (which altered ecological zones fragmenting continuous ranges) that rapid lineage diversification and expansion began within *C. hispidus* (see above).

Previous morphological accounts of *C. hispidus* report that many physical characteristics used to delimit subspecies may be too variable to be of taxonomic value. For example, hispid pocket mice found in Vernon Parish, Louisiana (*C. h. hispidus*; locality 25; Fig. 1) were characterized as more similar morphologically to *C. h. paradoxus* from the western portion of the species range than to other representatives of *C. h. hispidus* (Glass 1947). Other species accounts (e.g., Osgood 1900) indicate that there is only a gradual gradation of morphological differences among *C. h. hispidus*, *C. h. paradoxus*, and *C. h. spilotus*. Morphological examination herein also supports lack of differentiation both among named subspecies and mitochondrial clades (Fig. 4). Thus, it appears that subspecific definitions based on morphological characters examined to date are not appropriate for *C. hispidus*. We propose that rather than basing subspecific definitions on inconsistent morphological variation, subspecies within *C. hispidus* should be recognized based on genetic data and geographic barriers with which the genetically defined clades are broadly concordant. Using genetic data to recognize subspecies is in agreement with previous subspecies definitions (Barrowclough 1982; Endler 1977; Lidicker 1960, 1962) and studies (Hafner et al. 2008; Hafner and Smith 2010; Hafner et al. 2009; Patton et al. 2008; Shipp-Pennock et al. 2005) and would result in biologically meaningful taxonomic designations.

We acknowledge that the subspecies recognized here are defined solely using mtDNA and that reliance on 1 type of marker is not ideal for taxonomic revisions because the phylogeny represents a gene tree rather than a species tree (Ballard and Whitlock 2004; Bazin et al. 2006; Edwards et al. 2005; Maddison 1997). Despite these concerns, mtDNA data are ideal to address phylogeographic questions, especially when the goal of the study is to examine taxonomic or geographic limits of recently evolved species (Zink and Barrowclough 2008). In these cases, it is exceedingly difficult to find a nuclear marker with enough variability to be informative. Fast-evolving nuclear markers, such as microsatellites and single-nucleotide polymorphisms, are currently unavailable for *C. hispidus* and are more appropriate for rigorous demographic analyses (Edwards and Beerli 2000) with greater sampling than what is available for the current study. In an effort to provide additional support for our findings based on mtDNA, we examined both morphology as well as a nuclear molecular marker. Unfortunately, morphology is conserved within *C. hispidus*, and thus uninformative, and our examination of a nuclear molecular marker (exon 1 of the interphotoreceptor retinoid-binding protein) for a subset of specimens of *C. hispidus* provided no resolution among taxa (data available upon request). Importantly, the geographic distribution of subspecies based on the mtDNA data presented herein is associated with postulated historical barriers, and thus is phylogeographically more meaningful than previous morphologically defined subspecies.

Herein, we recognize 3 of the 4 mitochondrial clades of *C. hispidus* as subspecies. In doing so, we place *C. h. spilotus* and *C. h. zacatecae* in synonomy with *C. h. paradoxus* and *C. h. hispidus*, respectively, and restore *C. h. conditi* (in agreement with Hoffmeister [1986] and Hoffmeister and Goodpaster [1954]). At this time, we recognize clade A as incertae sedis. Although it is a genetically distinct group based on mitochondrial data (with 7, 8, and 17 unique nucleotides for COIII, *Cytb*, and ND2, respectively [Figs. 2 and 3]), support for this group is oftentimes low. Furthermore, the sample size for both molecular and morphological work for this clade is small to none ($n = 3$ and $n = 0$, respectively). Additional sampling and a thorough morphological and molecular investigation of hispid pocket mice from this region in central Mexico is necessary to determine the taxonomic status of clade A.

Chaetodipus Merriam, 1889

Perognathus Merriam, 1889:5. Part.

Chaetodipus Merriam, 1889. Type species *Perognathus spinatus* Merriam, 1889. *Chaetodipus* was regarded as a subgenus of *Perognathus*. Subgenus elevated to generic level by Hafner and Hafner (1983:24).

Burtognathus Hoffmeister, 1986. Type species *Chaetodipus hispidus* Baird, 1858, by original designation. Erected as a subgenus to include only *C. hispidus*. Regarded as a junior synonym of *Chaetodipus* by Patton (2005).

The genus *Chaetodipus* currently contains 17 or 18 species (Álvarez-Castañeda and Rios 2011; Patton 2005) distributed throughout the western United States and Mexico. Williams et al. (1993) provide a key to the Recent species of *Chaetodipus*.

Chaetodipus hispidus (Baird, 1858)
Hispid Pocket Mouse
(synonymy under subspecies)

Description.—Body size large for the genus, total length usually larger than 180 mm and length of the hind foot usually greater than 22 mm. Differs from other *Chaetodipus* species in having a noncrested tail equal to or shorter than the length of the head and body. Most similar to *C. baileyi*, but with coarser dorsal fur, fur with more buff to ochraceous tones, and with a conspicuous buff to ochraceous lateral stripe. Osgood (1900)

noted that the skull of *C. hispidus* varies individually more than is usual in the genus and affords scarcely any reliable differences among subspecies (Osgood 1900).

Distribution.—Occupies the Great Plains from south-central North Dakota southward to central Tamaulipas, Mexico, and westward to southeastern Arizona (Fig. 5). Occurs generally east of the Rocky Mountains (extending as far east as west-central Louisiana) and west of the Missouri River and Ozark Plateau (extending across southern New Mexico to southeastern Arizona and extreme northeastern Sonora). The southernmost limit of the range of *C. hispidus* is on the central plateau of Mexico (broadly, from southern Coahuila and Nuevo León southward through Zacatecas, Aguascalientes, eastern Jalisco, eastern San Luis Potosí, Querétaro, and Guanajuato, possibly extending as far south as Hidalgo).

Chaetodipus hispidus hispidus (Baird, 1858)

Perognathus hispidus hispidus Baird, 1858:421. Type locality "Charco Escondido, [Tamaulipas], México." Type specimen adult female, skin and skull (broken), United States National Museum number USNM 577, collected by D. N. Couch on 14 July 1853.

Perognathus hispidus zacatecae Osgood, 1900:45. Type locality "Valparaiso, Zacatecas, México." Type specimen adult female, skin and skull (broken), United States National Museum number USNM 91877, collected by E. A. Goldman on 16 December 1897.

C[*haetodipus*]. *h*[*ispidus*]. *hispidus*: Paulson, 1988:1. First use of current name combination.

C[*haetodipus*]. *h*[*ispidus*]. *zacatecae*: Paulson, 1988:1. Name combination.

Referred material.—Presented in Appendixes I and II and Fig. 1.

Description.—External characters as per the species. Means and ranges (in parentheses) of several skull characters (in mm) from specimens examined in Appendix II were: ONL, 28.96 (25.49–32.21); OIL, 26.02 (23.44–28.77); IOC, 7.23 (6.08–8.86); ZB, 13.77 (11.52–15.97); CW, 13.85 (12.31–15.59); MB, 12.95 (10.98–14.43); DIA, 6.86 (5.56–8.39).

Distribution.—Southern Texas, south of the Balcones Escarpment southward into northeastern Coahuila and Nuevo León, and south-central Tamaulipas, extending across the Sierra Madre Oriental onto the central plateau of Mexico. Within Mexico, northwestern limits are east-central Durango and north-central limits are southern Coahuila and probably southwestern Nuevo León with a northern limit south of the Southern Coahuila filter-barrier at the Río Nazas in Durango (Petersen 1976). Range extends southward through Zacatecas, San Luis Potosí, Aguascalientes, eastern Jalisco, Guanajuato, Querétaro, and probably México and Hidalgo. Complete distribution limits currently are unknown (see below).

Comments and comparisons with other taxa.—*Chaetodipus h. hispidus* is equivalent to clade C as defined genetically in this report (Figs. 2, 3, and 5). Morphologically, skull measurements are most similar to those of *C. h. conditi*. The geographic range defined herein is very different from that described in earlier accounts. The Balcones Escarpment and Gulf Coast marine incursions (resulting from climatic oscillations in southeastern Texas) may have served as barriers isolating *C. h. hispidus* from *C. h. paradoxus* to the north. Additionally, now included within *C. h. hispidus* are populations previously defined as *C. h. zacatecae*. Although Osgood (1900) and Glass (1947) noted apparent morphological differences between *C. h. zacatecae* and other subspecies of *C. hispidus*, our analysis of cranial characters does not agree with these findings. Furthermore, genetic data do not support the contention that *C. h. zacatecae* represents a distinct evolutionary lineage. Rather, individuals occupying the range of *C. h. zacatecae* group with *C. h. hispidus* due to apparent gene flow through the Sierra Madre Oriental (size and number of dispersal routes are unknown). The Southern Coahuila filter-barrier, however, does appear to serve as a northern limit between *C. h. hispidus* and clade A (incertae sedis). It is important to note that the full distribution of *C. h. hispidus* is not finalized. The western limits of the distribution of *C. h. hispidus* are unknown and it is possible that *C. h. hispidus* and *C. h. conditi* may be in contact provided appropriate grassland habitat (however, there appears to be very little gene flow between these 2 subspecies [Table 2]). Additional collections in Durango (west and north of the Southern Coahuila filter-barrier) as well as central Mexico are necessary to determine the full extent of the range of this subspecies. We did attempt to obtain a better idea of the full distribution of clade C by gathering sequence data from 1 museum skin snip specimen located in Hidalgo (one of the southernmost states where *C. h. zacatecae* has been previously collected). Unfortunately, due to a large amount of missing data we did not include this specimen in our analyses (skin snip samples were analyzed only if we had obtained at least 3 gene fragments, see "Materials and Methods"). Inclusion of this specimen in preliminary phylogenetic analyses, however, resulted in this specimen grouping with clade C, supporting our distribution map (Fig. 3).

Diagnosis.—*Chaetodipus h. hispidus* is currently diagnosable only by geography and mitochondrial data. This subspecies is recognized as a genetically distinct group based on 3 mitochondrial genes with 3, 1, and 8 unique nucleotides for COIII, *Cytb*, and ND2, respectively (Figs. 2 and 3).

Chaetodipus hispidus conditi (Allen, 1894)

Perognathus hispidus conditi Allen, 1894:318. Type locality "San Bernardino Ranch, southeastern corner of Cochise Co., Arizona." Type specimen adult male, skin and skull, American Museum of Natural History number AMNH 8360/6686, collected by B. C. Condit on 23 March 1894.

C[*haetodipus*]. *h*[*ispidus*]. *conditi*: Paulson, 1988:1. First use of current name combination.

Referred material.—Presented in Appendixes I and II and Fig. 1.

Description.—External characters as per the species. Means and ranges (in parentheses) of several skull characters (in mm) from specimens examined in Appendix II were: ONL, 29.20 (25.29–32.27); OIL, 26.04 (22.62–28.32); IOC, 6.91 (5.87–7.65); ZB, 13.78 (11.46–15.27); CW, 13.89 (12.23–15.00); MB, 13.26 (11.96–14.14); DIA, 6.90 (5.70–8.16).

Distribution.—Chihuahuan Desert from southwestern New Mexico and southeastern Arizona south through central Chihuahua and north-central Durango. The distribution of *C. h. conditi* also may extend into the extreme northeastern corner of Sonora.

Comments and comparisons with other taxa.—*Chaetodipus h. conditi* is equivalent to clade B as defined genetically herein (Figs. 2, 3, and 5). When he described *C. h. conditi*, Allen (1894) recognized that this subspecies could not be readily distinguished from *C. h. paradoxus*, hence its placement as a synonym of *C. h. paradoxus* by Hall (1981), among others. Hoffmeister (1986) and Hoffmeister and Goodpaster (1954), however, found morphologically distinguishable populations of *C. h. paradoxus* and *C. h. conditi* in Arizona and Chihuahua. Genetic data presented herein further support recognition of these western populations as a valid subspecies, *C. h. conditi*. The northeastern limit of the range of *C. h. conditi* is unknown, and this subspecies may contact *C. h. paradoxus* in this region. The Deming Plains and the Río Grande may serve as potential barriers between *C. h. conditi* and *C. h. paradoxus* and it is likely that contact between these 2 subspecies will depend on the presence of suitable grassland habitat. Additionally, the southeastern limit of the range of *C. h. conditi* also is unknown and it is possible that *C. h. conditi* and *C. h. hispidus* may be in contact provided appropriate grassland habitat (although there appears to be very little gene flow between these 2 subspecies [Table 2]). We note that repeated attempts to amplify genetic data from the type specimen failed. However, the specimens from localities 14, 15, 28, and 29 (Fig. 1 and Appendix I) were collected in the same or nearby counties as the type locality.

Diagnosis.—*Chaetodipus h. conditi* is currently diagnosable only by geography and mitochondrial data. This subspecies is recognized as a genetically distinct group based on 3 mitochondrial genes with 4, 1, and 5 unique nucleotides for COIII, *Cytb*, and ND2, respectively (Figs. 2 and 3).

Chaetodipus hispidus paradoxus (Merriam, 1889)

Perognathus hispidus paradoxus Merriam, 1889:24. Type locality "Banner, Trego County, Kansas." Type specimen adult female, skin and skull, United States National Museum number USNM 186513, collected by A. B. Baker on 17 October 1884.

Perognathus hispidus spilotus Merriam, 1889:25. Type locality "Gainesville, Cooke County, Texas."

Perognathus hispidus latirostris Rhoads, S. N. 1894:185. Type locality "Rocky Mountains."

Perognathus hispidus maximus Elliot, 1903:253. Type locality "Noble, Cleveland County, Oklahoma."

C[*haetodipus*]. *h*[*ispidus*]. *paradoxus*: Paulson, 1988:1. First use of current name combination.

C[*haetodipus*]. *h*[*ispidus*]. *spilotus*: Paulson, 1988:1. Name combination.

C[*haetodipus*]. *h*[*ispidus*]. *latirostris*: Paulson, 1988:1. Name combination.

C[*haetodipus*]. *h*[*ispidus*]. *maximus*: Paulson, 1988:1. Name combination.

Referred material.—Presented in Appendixes I and II and Fig. 1.

Description.—External characters as per the species. Means and ranges (in parentheses) of several skull characters (in mm) from specimens examined in Appendix II were: ONL, 30.32 (25.00–39.41); OIL, 27.21 (22.66–37.44); IOC, 7.24 (6.07–8.71); ZB, 14.52 (11.58–16.80); CW, 14.20 (12.46–15.91); MB, 13.23 (10.23–14.81); DIA, 7.08 (5.45–8.55).

Distribution.—Short and mixed grasslands of the northern and western Great Plains, generally west of the Missouri River, east of the Rocky Mountains, and north of the Balcones Escarpment of Texas. Distribution includes south-central North Dakota, eastern Colorado, South Dakota, Nebraska, Oklahoma, eastern and central New Mexico, and Texas north of the Balcones Escarpment extending eastward into west-central Louisiana.

Comments and comparisons with other taxa.—*Chaetodipus h. paradoxus* is equivalent to clade D as defined genetically in this report (Figs. 2, 3, and 5). Morphologically, *C. h. paradoxus* is the largest subspecies based on skull measurements. In previous taxonomic accounts, there were reports of considerable morphological intergradation in terms of size, color, and other characters among *C. h. hispidus*, *C. h. paradoxus* (and synonyms), and *C. h. spilotus*, resulting in multiple taxonomic changes. Past taxonomic confusion as a result of morphological intergradation is appropriately dealt with by redefining the geographic ranges of *C. h. hispidus* and *C. h. paradoxus*, and recognizing *C. h. spilotus* as a synonym of *C. h. paradoxus*. The current geographic range of *C. h. paradoxus* encompasses the range previously described for *C. h. spilotus* and the northern and eastern parts of the range previously described for *C. h. hispidus*. The western limits of the range are unknown and *C. h. paradoxus* may come into contact with *C. h. conditi*. However, it is likely that the Río Grande and suitable habitat within the Deming Plains will determine the western limits of *C. h. paradoxus*.

Diagnosis.—*Chaetodipus h. paradoxus* is currently diagnosable only by geography and mitochondrial data. This subspecies is recognized as a genetically distinct group based on 2 unique nucleotides for ND2 (Figs. 2 and 3).

Resumen

El ratón *Chaetodipus hispidus* es uno de los miembros más divergentes genéticamente y morfológicamente dentro de los heterómidos del género *Chaetodipus*. Existen 4 subespecies de *C. hispidus* reconocidos, *C. h. hispidus*, *C. h. paradoxus*, *C. h. spilotus*, y *C. h. zacatecae*, cuya distribución se extiende desde Dakota del Norte hacia el sur por las Grandes Llanuras y Texas hasta el centro de México. En este estudio, se investigó la

estructura filogeográfica de *C. hispidus* através del examen de datos de ADN mitocondrial en muestras recientes y antiguas a lo largo de las zonas de la distribución de las especies. También se examinaron 11 caracteres craneales en 303 muestras para determinar la variación morfológica en las especies. Aunque los análisis no pudieron diferenciar entre las subespecies, los análisis filogenéticos indican que 4 subespecies actualmente reconocidas de *C. hispidus* no son genéticamente distintos. En cambio, nuestros resultados indican que hay 4 nuevos clados mitocondriales distintos de *C. hispidus* que no corresponden con las subespecies actualmente reconocidas, pero cuyos límites geográficos coinciden con grandes rasgos geográficos delsur de los Estados Unidos y el norte de México. La barrera-filtro de Coahuila Meridional (Durango y Coahuila), las llanuras de Deming (Nuevo México), y el escarpado de Balcones (Texas) han actuado probablemente como barreras físicas intermitentes al flujo genético entre los distintos clados mitocondriales, los cuales reconocemos como subespecies dentro de *C. hispidus*.

Acknowledgments

We thank the following institutions and curators for providing tissue samples: American Museum of Natural History (R. Voss), Angelo State Natural History Collections (L. Ammerman and M. Tipps), Louisiana State University Museum of Natural Science (R. Brumfield and D. Dittman), Natural Science Research Laboratory at the Museum of Texas Tech University (R. Baker and H. Garner), New Mexico Museum of Natural History (G. Morgan and P. Gegick), Sam Noble Oklahoma Museum of Natural History (J. Braun), University of Kansas Natural History Museum (R. Timm), University of New Mexico Museum of Southwestern Biology (J. Cook and C. Parmenter), and University of Nevada Las Vegas (B. Riddle and S. Neiswenter). We are especially grateful to R. Timm and J. Braun for hosting JEL's visits to their collections during a blizzard. P. Sudman, B. Tanis, G. Wilson, and R. Voss helped to find voucher specimen information and A. Leaché provided a map of North America. We are indebted to D. Hafner and M. Hafner and 4 anonymous reviewers for providing valuable and insightful comments on earlier drafts of this manuscript. The Conway, Light, and Voelker laboratories at Texas A&M University also provided helpful feedback on the manuscript. We thank J. A. Harvey and M. Palacios for providing a Spanish translation of the abstract. We acknowledge the Texas A&M University Brazos HPC Cluster that contributed to the research reported here (brazos.tamu.edu). This is publication 1424 of the Texas Cooperative Wildlife Collection and publication 204 of the Center for Biosystematics and Biodiversity, both at Texas A&M University.

Literature Cited

Alexander, L. F., and B. R. Riddle. 2005. Phylogenetics of the New World rodent family Heteromyidae. Journal of Mammalogy 86:366–379.

Allen, J. A. 1894. Descriptions of ten new North American mammals, and remarks on others. Bulletin of the American Museum of Natural History 6:317–332.

Álvarez-Castañeda, S. T., and E. Rios. 2011. Revision of *Chaetodipus arenarius* (Rodentia: Heteromyidae). Zoological Journal of the Linnean Society 161:213–228.

Amman, B. R., and R. D. Bradley. 2004. Molecular evolution in *Baiomys* (Rodentia: Sigmodontinae): evidence for a genetic subdivision in *B. musculus*. Journal of Mammalogy 85:162–166.

Anducho-Reyes, M. A., A. I. Cognato, J. L. Hayes, and G. Zuniga. 2008. Phylogeography of the dark beetle *Dendroctonus mexicanus* Hopkins (Coleoptera: Curculionidae: Scolytinae). Molecular Phylogenetics and Evolution 49:930–940.

Arriaga, L., C. Aguilar, D. Espinosa-Organista, and R. Jiménez. 1997. Regionalización ecológica y biogeográfica de México. Taller de la Comisión Nacional para el Conocimiento y Uso de la Biodiversidad (CONABIO), México, Distrito Federal, México.

Baird, S. F. 1858. Mammals. Pp. 1–757 in Reports of explorations and surveys, to ascertain the most practical and economical route for a railroad from the Mississippi River to the Pacific Ocean. O. P. Nicholson Printer, Washington, D.C. Vol. 8. Pt. 1.

Baker, R. H. 1956. Mammals of Coahuila, México. University of Kansas Publications, Museum of Natural History 9:125–335.

Ballard, J. W. O., and M. C. Whitlock. 2004. The incomplete natural history of mitochondria. Molecular Ecology 13:729–744.

Barrowclough, G. F. 1982. Geographic variation, predictiveness, and subspecies. Auk 99:601–603.

Bazin, E., S. Glemin, and N. Galtier. 2006. Population size does not influence mitochondrial genetic diversity in animals. Science 312:570–572.

Best, T. L. 1993. Patterns of morphologic and morphometric variation in heteromyid rodents. Pp. 197–235 in Biology of the Heteromyidae (H. H. Genoways and J. H. Brown, eds.). Special Publication 10, The American Society of Mammalogists.

Bradley, R. D., D. S. Carroll, M. L. Haynie, R. M. Martínez, M. J. Hamilton, and C. W. Kilpatrick. 2004. A new species of *Peromyscus* from western Mexico. Journal of Mammalogy 85:1184–1193.

Brown, J. M., and A. R. Lemmon. 2007. The importance of data partitioning and the utility of Bayes factors in Bayesian phylogenetics. Systematic Biology 56:643–655.

Burbrink, F. T. 2001. Systematics of the eastern ratsnake complex (*Elaphe obsoleta*). Herpetological Monographs 15:1–53.

Cassens, I., K. Van Waerebeck, P. B. Best, E. A. Crespo, J. Reyes, and M. C. Milinkovitch. 2003. The phylogeography of dusky dolphins (*Lagenorhynchus obscurus*): a critical examination of network methods and rooting procedures. Molecular Ecology 12:1781–1792.

Castoe, T. A., C. L. Spencer, and C. L. Parkinson. 2007. Phylogeographic structure and historical demography of the western diamondback rattlesnake (*Crotalus atrox*): a perspective on North American desert biogeography. Molecular Phylogenetics and Evolution 42:193–212.

Ceballos, G., J. Arroyo-Cabrales, and E. Ponce. 2010. Effects of Pleistocene environmental changes on the distribution and community structure of the mammalian fauna of Mexico. Quaternary Research 73:464–473.

Clement, M., D. Posada, and K. A. Crandall. 2000. TCS: a computer program to estimate gene genealogies. Molecular Ecology 9:1657–1659.

Corruccini, R. S. 1975. Multivariate analysis in biological anthropology: some considerations. Journal of Human Evolution 4:1–19.

Crandall, K. A. 1996. Multiple interspecies transmissions of human and simian T-cell leukemia/lymphoma virus type I sequences. Molecular Biology and Evolution 13:115–131.

Crandall, K. A., and A. R. Templeton. 1996. Applications of intraspecific phylogenetics. Pp. 81–99 in New uses for new

phylogenies (P. H. Harvey, A. J. Leigh Brown, J. Maynard Smith, and S. Nee, eds.). Oxford University Press, New York.

Demboski, J. R., and J. Sullivan. 2003. Extensive mtDNA variation within the yellow-pine chipmunk, *Tamias amoenus* (Rodentia: Sciuridae), and phylogeographic inferences for northwest North America. Molecular Phylogenetics and Evolution 26:389–408.

Dicken, S. N. 1936. The Basin settlements of the Middle Sierra Madre Oriental, Mexico. Annals of the Association of American Geographers 26:157–178.

dos Reis, S. F., L. M. Pessoa, and R. E. Strauss. 1990. Application of size-free canonical discriminant analysis to studies of geographic differentiation. Brazilian Journal of Genetics 13:509–520.

Drummond, A., S. Ho, M. Phillips, and A. Rambaut. 2006. Relaxed phylogenetics and dating with confidence. PLoS Biology 4:699–710.

Drummond, A., and A. Rambaut. 2007. BEAST: Bayesian evolutionary analysis by sampling trees. BMC Evolutionary Biology 7:214.

Dupanloup, L., S. Schneider, and L. Excoffier. 2002. A simulated annealing approach to define the genetic structure of populations. Molecular Ecology 11:2571–2581.

Edwards, S. V., and P. Beerli. 2000. Perspective: gene divergence, population divergence, and the variance in coalescence time in phylogeographic studies. Evolution 54:1839–1854.

Edwards, S. V., et al. 2005. Speciation in birds: genes, geography and sexual selection. Proceedings of the National Academy of Sciences 102:6550–6557.

Elliot, D. G. 1903. Descriptions of twenty-seven apparently new species and subspecies of mammals. Field Columbian Museum, Zoölogical Series 87:239–332.

Endler, J. A. 1977. Geographic variation, speciation, and clines. Monographs in Population Biology 10:1–246.

Excoffier, L., G. Laval, and S. Schneider. 2005. Arlequin (version 3.0): an integrated software package for population genetics data analysis. Evolutionary Bioinformatics Online 1:47–50.

Excoffier, L., P. E. Smouse, and J. M. Quattro. 1992. Analysis of molecular variance inferred from metric distances among DNA haplotypes: application to human mitochondrial DNA restriction data. Genetics 131:479–491.

Fa, J. E., and L. M. Morales. 1993. Patterns of mammalian diversity in Mexico. Pp. 319–361 in Biological diversity of Mexico: origins and distribution (T. P. Ramamoorthy, R. Bye, A. Lot, and J. Fa, eds.). Oxford University Press, New York.

Felsenstein, J. 1985. Phylogenies from gene-frequencies—a statistical problem. Systematic Zoology 34:300–311.

Fu, Y. X. 1997. Statistical tests of neutrality of mutations against population growth, hitchhiking and background selection. Genetics 147:915–925.

Gehlbach, F. R. 1991. The east–west transition zone of terrestrial vertebrates in central Texas: a biogeographical analysis. Texas Journal of Science 43:415–427.

Geluso, K., and G. D. Wright. 2010. Hispid pocket mouse (*Chaetodipus hispidus*) in east-central and northeastern Nebraska. Western North American Naturalist 70:126–129.

Glass, B. P. 1947. Geographic variation in *Perognathus hispidus*. Journal of Mammalogy 28:174–179.

Gould, S. J. 1966. Allometry and size in ontogeny and phylogeny. Biological Review 41:587–640.

Guevara-Chumacero, L. M., R. López-Wilchis, F. F. Pedroche, J. Juste, C. Ibáñez, and I.D.L.A. Barriga-Sosa. 2010. Molecular phylogeography of *Pteronotus davyi* (Chiroptera: Mormoopidae) in Mexico. Journal of Mammalogy 91:220–232.

Hafner, D. J., M. S. Hafner, G. L. Hasty, T. A. Spradling, and J. W. Demastes. 2008. Evolutionary relationships of pocket gophers (*Cratogeomys castanops* species group) of the Mexican Altiplano. Journal of Mammalogy 89:190–208.

Hafner, D. J., and B. R. Riddle. 2005. Mammalian phylogeography and evolutionary history of northern Mexico's deserts. Pp. 225–245 in Biodiversity, ecosystems, and conservation in northern Mexico (J.-L. E. Cartron, G. Ceballos, and R. S. Felger, eds.). Oxford University Press, New York.

Hafner, D. J., and B. R. Riddle. 2011. Boundaries and barriers of North American warm deserts: an evolutionary perspective. Pp. 75–114 in Palaeogeography and palaeobiogeography: biodiversity in space and time (P. Upchurch, A. J. McGowan, and C. S. C. Slater, eds.). CRC Press, Boca Raton, Florida.

Hafner, D. J., and A. T. Smith. 2010. Revision of the subspecies of the American pika, *Ochotona princeps* (Lagomorpha: Ochotonidae). Journal of Mammalogy 91:401–417.

Hafner, J. C., and M. S. Hafner. 1983. Evolutionary relationships of heteromyid rodents. Great Basin Naturalist Memoirs 7:3–29.

Hafner, J. C., et al. 2007. Basal clades and molecular systematics of heteromyid rodents. Journal of Mammalogy 88:1129–1145.

Hafner, M. S., D. J. Hafner, J. W. Demastes, G. L. Hasty, J. E. Light, and T. A. Spradling. 2009. Evolutionary relationships of pocket gophers of the genus *Pappogeomys* (Rodentia: Geomyidae). Journal of Mammalogy 90:47–56.

Hall, E. R. 1981. The mammals of North America. 2nd ed. John Wiley & Sons, Inc., New York.

Hoffmeister, D. F. 1986. Mammals of Arizona. University of Arizona Press, Tucson.

Hoffmeister, D. F., and W. W. Goodpaster. 1954. The mammals of the Huachuca Mountains, southeastern Arizona. Illinois Biological Monographs 24:1–152.

Huelsenbeck, J. P., and B. Rannala. 1997. Phylogenetic methods come of age: testing hypotheses in an evolutionary context. Science 276:227–232.

Huelsenbeck, J. P., and F. Ronquist. 2001. MrBayes: Bayesian inference of phylogeny. Bioinformatics 17:754–755.

Hunt, C. B. 1983. Physiographic overview of our arid lands in the western U.S. Pp. 7–61 in Origin and evolution of deserts (S. G. Welss and D. R. Haragan, eds.). University of New Mexico Press, Albuquerque.

Jezkova, T., J. R. Jaegar, Z. L. Marshall, and B. R. Riddle. 2009. Pleistocene impacts on the phylogeography of the desert pocket mouse (*Chaetodipus penicillatus*). Journal of Mammalogy 90:306–320.

Kerhoulas, N. J., and B. S. Arbogast. 2010. Molecular systematics and Pleistocene biogeography of Mesoamerican flying squirrels. Journal of Mammalogy 91:654–667.

Lack, J. B., R. S. Pfau, and G. M. Wilson. 2010. Demographic history and incomplete lineage sorting obscure population genetic structure of the Texas mouse (*Peromyscus attwateri*). Journal of Mammalogy 91:314–325.

Lidicker, W. Z., Jr. 1960. An analysis of intraspecific variation in the kangaroo rat *Dipodomys merriami*. University of California Publications in Zoology 67:125–218.

Lidicker, W. Z., Jr. 1962. The nature of subspecies boundaries in a desert rodent and its implications for subspecies taxonomy. Systematic Zoology 11:160–171.

LIGHT, J. E., AND D. L. REED. 2009. Multigene analysis of phylogenetic relationships and divergence times of primate sucking lice (Phthiraptera: Anoplura). Molecular Phylogenetics and Evolution 50:376–390.

MADDISON, W. P. 1997. Gene trees in species trees. Systematic Biology 46:523–536.

MCCORMACK, J. E., A. T. PETERSON, E. BONACCORSO, AND T. B. SMITH. 2008. Speciation in the highlands of Mexico: genetic and phenotypic divergence in the Mexican jay (*Aphelocoma ultramarina*). Molecular Ecology 17:2505–2521.

MCKNIGHT, M. L. 2005. Phylogeny of the *Perognathus longimembris* species group based on mitochondrial cytochrome-*b*: how many species? Journal of Mammalogy 86:826–832.

MERRIAM, C. H. 1889. Revision of the North American pocket mice. North American Fauna 1:1–29.

MILLER, M. P. 2005. Alleles In Space (AIS): computer software for the joint analysis of interindividual spatial and genetic information. Journal of Heredity 96:722–724.

MORAFKA, D. J. 1977. A biogeographical analysis of the Chihuahuan Desert through its herpetofauna. Dr. W. Junk B.V., Publishers, The Hague, Netherlands.

MORRONE, J. J. 2005. Hacia una síntesis biogeográfica de México. Revista Mexicana de Biodiversidad 76:207–252.

NEISWENTER, S. A., AND B. R. RIDDLE. 2010. Diversification of the *Perognathus flavus* species group in emerging arid grasslands of western North America. Journal of Mammalogy 91:348–362.

NYLANDER, J. A. A., F. RONQUIST, J. P. HUELSENBECK, AND J. L. NIEVES-ALDREY. 2004. Bayesian phylogenetic analysis of combined data. Systematic Biology 53:47–67.

OSGOOD, W. H. 1900. Revision of the pocket mice of the genus *Perognathus*. North American Fauna 18:1–65.

PATTON, J. L. 2005. Family Heteromyidae. Pp. 844–858 in Mammal species of the world: a taxonomic and geographic reference (D. E. Wilson and D. M. Reeder, eds.). 3rd ed. Johns Hopkins University Press, Baltimore, Maryland.

PATTON, J. L., D. G. HUCKABY, AND S. T. ÁLVAREZ-CASTAÑEDA. 2008. The evolutionary history and a systematic revision of woodrats of the *Neotoma lepida* group. University of California Publications in Zoology 135:1–472.

PATTON, J. L., AND D. S. ROGERS. 1993. Cytogenetics. Pp. 236–258 in Biology of the Heteromyidae (H. H. Genoways and J. H. Brown, eds.). Special Publication 10, The American Society of Mammalogists.

PATTON, J. L., S. W. SHERWOOD, AND S. Y. YANG. 1981. Biochemical systematics of chaetodipine pocket mice, genus *Perognathus*. Journal of Mammalogy 62:477–492.

PAULSON, D. D. 1988. *Chaetodipus hispidus*. Mammalian Species 320:1–4.

PETERSEN, M. K. 1976. The Rio Nazas as a factor in mammalian distribution in Durango, Mexico. Southwestern Naturalist 20:495–502.

POSADA, D., AND T. R. BUCKLEY. 2004. Model selection and model averaging in phylogenetics: advantages of Akaike information criterion and Bayesian approaches over likelihood ratio tests. Systematic Biology 53:793–808.

POSADA, D., AND K. A. CRANDALL. 1998. ModelTest: testing the model of DNA substitution. Bioinformatics 14:817–818.

RAMBAUT, A. 1996. Se-Al, sequence alignment editor. Version 2.01all.

RAMBAUT, A. 2008. FigTree, version 1.31.

RAMBAUT, A., AND A. DRUMMOND. 2004. TRACER, version 1.5.

RAY, N., M. CURRAT, AND L. EXCOFFIER. 2003. Intra-deme molecular diversity in spatially expanding populations. Molecular Biology and Evolution 20:76–86.

RHOADS, S. N. 1894. Description of a new *Perognathus* collected by J. K. Townsend in 1834. American Naturalist 28:185–187.

RIDDLE, B. R. 1995. Molecular biogeography in the pocket mice (*Perognathus* and *Chaetodipus*) and grasshopper mice (*Onychomys*): the late Cenozoic development of a North American aridlands rodent guild. Journal of Mammalogy 76:283–301.

RIDDLE, B. R., AND D. J. HAFNER. 2006. A step-wise approach to integrating phylogeographic and phylogenetic biogeographic perspectives on the history of a core North American warm deserts biota. Journal of Arid Environments 66:434–461.

RIDDLE, B. R., D. J. HAFNER, AND L. F. ALEXANDER. 2000a. Phylogeography and systematics of the *Peromyscus eremicus* species group and the historical biogeography of North American warm regional deserts. Molecular Phylogenetics and Evolution 17:145–160.

RIDDLE, B. R., D. J. HAFNER, L. F. ALEXANDER, AND J. R. JAEGER. 2000b. Cryptic vicariance in the historical assembly of a Baja California peninsular desert biota. Proceedings of the National Academy of Sciences 97:14438–14443.

RIDDLE, B. R., AND R. L. HONEYCUTT. 1990. Historical biogeography in North American arid regions: an approach using mitochondrial DNA phylogeny in grasshopper mice (genus *Onychomys*). Evolution 44:1–15.

ROGERS, A. R., AND H. HARPENDING. 1992. Population growth makes waves in the distribution of pairwise genetic differences. Molecular Biology 9:552–569.

RONQUIST, F., AND J. P. HUELSENBECK. 2003. MrBayes 3: phylogenetic inference under mixed models. Bioinformatics 19:1572–1574.

ROZAS, J., J. C. SÁNCHEZ-DELBARRIO, X. MESSEGUER, AND R. ROZAS. 2003. DnaSP, DNA polymorphism analyses by the coalescent and other methods. Bioinformatics 19:2496–2497.

SCHMIDLY, D. J. 1974. Factors governing the distribution of mammals in the Chihuahuan Desert region. Pp. 163–192 in Transactions of the Symposium on the Biological Resources of the Chihuahuan Desert Region, United States and Mexico (R. H. Wauer and D. H. Riskand, eds.). National Park Service Transactions and Proceedings Series 3:1–658.

SHIPP-PENNOCK, M. A., W. D. WEBSTER, AND D. W. FRESHWATER. 2005. Systematics of the white-footed mouse (*Peromyscus leucopus*) in the mid-Atlantic region. Journal of Mammalogy 86:803–813.

SMITH, H. M., AND H. K. BUECHNER. 1947. The influence of the Balcones Escarpment on the distribution of amphibians and reptiles in Texas. Bulletin of the Chicago Academy of Sciences 8:1–16.

SMITH, M. F., AND J. L. PATTON. 1991. Variation in mitochondrial cytochrome *b* sequence in natural populations of South American akodontine rodents (Muridae: Sigmodontinae). Molecular Biology and Evolution 8:85–103.

SORENSON, M. D., J. C. AST, D. E. DIMCHEFF, T. YURI, AND D. P. MINDELL. 1999. Primers for a PCR-based approach to mitochondrial genome sequencing in birds and other vertebrates. Molecular Phylogenetics and Evolution 12:105–114.

SPSS INC. 1996. SYSTAT 8.0 statistics. SPSS Inc., Chicago, Illinois.

STAMATAKIS, A. 2006. RAxML-VI-HPC: maximum likelihood-based phylogenetic analyses with thousands of taxa and mix models. Bioinformatics 22:2688–2690.

SWOFFORD, D. L. 2003. PAUP*: phylogenetic analysis using parsimony (*and other methods). Version 4. Sinauer Associates, Inc., Publishers, Sunderland, Massachusetts.

TAJIMA, F. 1989. Statistical method for testing the neutral mutation hypothesis by DNA polymorphism. Genetics 123:585–595.

TEMPLETON, A. R., K. A. CRANDALL, AND C. F. SING. 1992. A cladistic analysis of phenotypic associations with haplotypes inferred from restriction endonuclease mapping and DNA sequence data. III. Cladogram estimation. Genetics 132:619–633.

WAHLERT, J. H. 1993. The fossil record. Pp. 1–37 in Biology of the Heteromyidae (H. H. Genoways and J. H. Brown, eds.). Special Publication 10, The American Society of Mammalogists.

WILLIAMS, D. F., H. H. GENOWAYS, AND J. K. BRAUN. 1993. Taxonomy. Pp. 38–196 in Biology of the Heteromyidae (H. H. Genoways and J. H. Brown, eds.). Special Publication 10, The American Society of Mammalogists.

ZINK, R. M., AND G. F. BARROWCLOUGH. 2008. Mitochondrial DNA under siege in avian phylogeography. Molecular Ecology 17:2107–2121.

Submitted 28 September 2011. Accepted 27 January 2012.

Associate Editor was Ryan W. Norris.

APPENDIX I

Hispid pocket mouse (*Chaetodipus hispidus*) taxa examined in the molecular section of this study. Skin snip samples from museum study skins are indicated with asterisks (*). Number of the locality is as in Fig. 1. Museum and other number abbreviations are as follows: Angelo State Natural History Collections (ASNHC and ASK); Centro de Investigaciones Biologicas del Noroeste, S.C. (CIB); Fort Hayes State University's Sternberg Museum (FHSU); Louisiana State University Museum of Natural Science (LSUMZ and M); Moore Laboratory of Zoology (MLZ); Natural Science Research Laboratory at the Museum of Texas Tech University (TTU and TK); New Mexico Museum of Natural History (NMMNH); Sam Noble Oklahoma Museum of Natural History (OMNH); The University of Kansas Natural History Museum (KU): University of New Mexico Museum of Southwestern Biology (MSB and NK): Texas Cooperative Wildlife Collection (TCWC and AK) and University of Nevada Las Vegas Tissue Collection (LVT).

Locality number and locality	Latitude	Longitude	Museum number	Other number
Mexico				
1. Chihuahua: 21 mi WSW Jiménez	27.037	−105.244	NMMNH 5377	
2. Chihuahua: 14 km E, 3 km N Pancho Villa	30.833	−108.5	MSB 60848	NK 17573
3. Coahuila: 5 km S, 16 km W General Cepeda	25.3308	−101.6224	NMMNH 4705	
			NMMNH 4704	LVT 6603
4. Coahuila: 2 mi E Agua Nueva	25.3382	−101.5846	NMMNH 4716	LVT 6627
5. Coahuila: 40 km SW Ciudad Acuna	29.31667	−100.9333	CIB 14536	
6. Coahuila: 5 km NW Villa Union	28.2167	−100.7166	CIB 14539	
7. Durango: 7 mi NNW La Zarca	25.9062	−104.6964	NMMNH 2545	LVT 1099
8. Guanajuato: 4 mi N, 5 mi W Leon*	21.18	−101.75	KU 48669	
9. Jalisco: Belen De Refugio*	21.52	−102.43	KU 103753	
10. Nuevo León: 2.5 mi W Linares*	24.85	−99.6	KU 88543	
11. Tamaulipas: 9.5 mi SW Padilla*	23.91	−98.88	KU 88544	
12. Zacatecas: 4.5 km NW Plateros	23.21667	−102.85	CIB 16674	
13. Zacatecas: 5.5 mi NW Juan Aldama*	24.34734	−103.4561	OMNH 9981	
United States				
14. Arizona: Cochise Co., 7 mi S, 4 mi E Portal	31.8139	−109.0597	ASNHC 12111	ASK 5380
15. Arizona: Pima Co., 10 mi NE Sonoita	32.1679	−111.7003	NMMNH 5806	LVT 9340
16. Colorado: Baca Co., Comanche Grasslands	37.25	−103.5	MSB 75121	NK 56022
17. Colorado: Weld Co.	40.6667	−104.3667	MSB 74660	NK 56093
18. Kansas: Jackson Co., 2 mi N, 2.5 mi E, Holton*	39.49	−95.68	KU 74689	
19. Kansas: Morris Co., 4.125 mi S, 6 mi W Council Grove*	38.6	−96.6	KU 99262	
20. Kansas: Pawnee Co., Fort Larned National Historic Site	38.1843	−99.2155	MSB 73902	NK 53298
21. Kansas: Pratt Co., 4 mi S, 0.5 mi W Cairo*	37.59	−98.56	KU 143929	
22. Kansas: Reno Co., Turon*	37.8	−98.42	KU 63219	
23. Kansas: Riley Co., Fort Riley*	39.6	−96.49	TCWC 50379	
24. Kansas: Washington Co., 7.75 mi N, 3 mi W Washington*	39.93	−97.12	KU 139195	
25. Louisiana: Vernon Parish, 1.5 km N, 11 km E Fort Polk	31.06	−93.0905	LSUMZ 23809	M-129
26. Nebraska: Cameron Co., 20 mi N Johnstown	42.8622	−100.0569	FHSU 35960	M-10694
27. Nebraska: Scotts Bluff Co., Scotts Bluff National Monument	41.8375	−103.706	MSB 73772	NK 53344
28. New Mexico: Hidalgo Co., Gray Ranch 1 mi S of Hwy 338	31.404	−108.865	MSB 140911	NK 40759
29. New Mexico: Hidalgo Co., Animas Valley, Middle Wells	31.6687	−108.8346	MSB 46000	NK 3724
30. New Mexico: Mora Co., 1.5 mi NW Wagon Mound	36.0243	−104.725	MSB 55811	NK 1186
31. New Mexico: Otero Co., Fort Bliss	32.2503	−105.876	TTU 76382	TK 51801
32. New Mexico: Roosevelt Co., Canon Air Force Base	34.0016	−103.6393	MSB 75825	NK 17005
33. New Mexico: Union Co., Kiowa National Grasslands	36.6074	−103.1012	MSB 58938	NK 8845
34. Oklahoma: Comanche Co., 3.6 mi S Cache	34.5768	−98.628	TTU 42045	TK 27124
35. Oklahoma: Haskell Co., 1.5 mi E Porum*	35.35621	−95.23896	OMNH 13963	
36. Oklahoma: Le Flore Co., 5 mi N, 2.5 mi E Bokoshe*	35.25902	−94.7416	OMNH 13980	
37. Oklahoma: Marshall Co., Lake Texoma*	33.8709	−96.85723	OMNH 15492	
38. Oklahoma: McClain Co., 5.6 mi S, 2 mi W Kessler Farm*	34.9777	−97.5197	OMNH 32504	
39. South Dakota: Pennington Co., 13 mi E Scenic	44.01	−102.5591	NMMNH 5784	LVT 9303

APPENDIX I.—Continued.

Locality number and locality	Latitude	Longitude	Museum number	Other number
40. South Dakota: Perkins Co., 2 mi S Shade Hill	44.4710	−102.48	NMMNH 5790	LVT 9312
41. Texas: Anderson Co., Gus Engeling Wildlife Management Area	31.9774	−95.8829	TTU 75422	TK 52093
42. Texas: Brown Co., Camp Bowie	31.67	−98.97	ASNHC 12513	ASK 6585
43. Texas: Cameron Co., Las Palomos Wildlife Management Area	26.3213	−97.8228	LSUMZ 36386	M-8160
44. Texas: Colorado Co., 2.5 mi E Weimar	29.701	−96.736	TTU 49404	TK 28596
45. Texas: Dimmit Co., 7.1 mi E Carrizo Springs	28.525	−99.74	MSB 57479	NK 6834
46. Texas: Dimmit Co., 13 mi W Artesia Wells	28.2914	−99.4855	ASNHC 11467	ASK 5037
47. Texas: Donley Co., 3.0 mi S, 1.5 mi W Clarendon	34.9364	−100.8911	TTU 100770	TK 119006
48. Texas: Duval Co., 3 mi N San Diego	27.805	−98.234	MSB 59017	NK 6842
49. Texas: Garza Co., 14 mi S, 1 mi E Post	32.987	−101.358	TTU 53317	TK 27281
50. Texas: Hidalgo Co., Mission	26.198	−98.35	LSUMZ 36375	M-7828
51. Texas: Irion Co., 7.6 mi N, 0.9 mi E Mertzon	31.37	−100.805	ASNHC 12770	ASK 5284
52. Texas: Irion Co., 2.4 mi S, 0.4 mi W Barnhart	31.098	−101.18	ASNHC 12775	ASK 5255
53. Texas: Jeff Davis Co., 2.5 mi S Ft. Davis	30.5567	−103.9394	MSB 85977	NK 42509
54. Texas: Jim Wells Co., La Copita Research Facility	27.8	−98.2078	MSB 88994	NK 44706
55. Texas: Kenedy Co., 25.3 mi S Rivieria	26.937	−97.7921	LSUMZ 36416	M-7886
56. Texas: Mason Co., Mason Mt. Wildlife Management Area	30.7478	−99.2319	TTU 107995	TK 119282
57. Texas: McLennan Co., Waco	33.335	−101.435	TTU 39806	TK 24660
58. Texas: Medina Co., D'Hanis, Rothe Ranch	29.33	−99.279	MSB 88995	NK 44742
59. Texas: Parker Co., 4.9 S, 4.4 mi E Weatherford	32.714	−97.7668	ASNHC 12044	ASK 5313
60. Texas: San Saba Co., 1 mi S, 10 mi W Richland Springs	31.257	−99.117	TTU 77147	TK 57937
61. Texas: Tom Green Co., San Angelo State Park	31.495	−100.53	ASNHC 11840	ASK 5175
62. Texas: Wilbarger Co., 16.2 mi S Vernon*	33.9194	−99.26508	OMNH 6819	
Outgroup taxa				
Chaetodipus baileyi				
United States: New Hidalgo Co., Doubtful Canyon, 8 mi N, 1 mi W Steins, 1,380 m			NMMNH 4421	
Chaetodipus formosus				
United States: California: San Bernardino Co., 8.9 mi N, 1.1 mi E Red Mountain, 3,150 ft			MLZ 1863	

APPENDIX II

The 303 specimens of *Chaetodipus hispidus* from 254 localities examined in morphological analyses are listed below by newly recognized subspecies, locality, and museum acronym. Locality numbers are given in parentheses. Collection acronyms are as follows: Sam Noble Oklahoma Museum of Natural History (OMNH), Texas Cooperative Wildlife Collection (TCWC), The University of Kansas Natural History Museum (KU), and United States National Museum of Natural History (USNM). Specimens in bold are type or topotype specimens. The type specimens of *C. h. hispidus* and *C. h. zacatecae* held at the USNM were damaged, and thus were not included in the analysis. No specimens of Clade A were available for measurement.

Chaetodipus hispidus hispidus (n = 80).—MÉXICO. (1) Coahuila: 7 mi S, 4 mi E Bella Unión (KU 48664); (2) Coahuila: 11 mi W Hacienda San Miguel (KU 35799); (3) Coahuila: 6 mi N, 2 mi E La Babia (KU 35806); (4) Coahuila: La Gacha (KU 57046); (5) Coahuila: 0.5 mi E Las Margaritas (KU 57045); (6) Coahuila: 1 mi W Las Margaritas (KU 57043); (7) Coahuila: 5 mi W Nadadores (KU 56620); (8) Coahuila: 2 mi S, 11 mi E Nava (KU 48652, KU 48655); (9) Coahuila: Cañon del Cochino, 16 mi N, 21 mi E Piedra Blanca (KU 35798); (10) Coahuila: 15 mi N, 8 mi W Piedras Negras (KU 35800); (11) Coahuila: Sabinas (USNM 117145); (12) Coahuila: 29 mi N, 6 mi E Sabinas (KU 35808); (13) Coahuila: 2 mi S, 3 mi E San Juan de Sabinas (KU 48659, KU 48663, KU 49633); (14) Guanajuato: Celaya (USNM 78423); (15) Guanajuato: 5 mi E Celaya (KU 48670, KU 48672, KU 48674); (16) Hidalgo: 85 km N México City (TCWC 3009, TCWC 3010, TCWC 3013, TCWC 3015); (17) Jalisco: Belén del Refugio (KU 103753, KU 103755); (18) Jalisco: 5 mi E Encarnación de Diaz (KU 107605); (19) Nuevo León: 15 mi N, 2 mi W Anáhuac (KU 56625); (20) Nuevo León: Río Salado, La Gloria (KU 55620); (21) Nuevo León: Linares (USNM 26578); (22) Nuevo León: 6 mi SW Montemorelos (KU 88540); (23) Nuevo León: Vallecillo (KU 55622); (24) Tamaulipas: Mier (USNM 27679); (25) Tamaulipas: Nuevo Laredo (USNM 116123); (26) Tamaulipas: 10 mi S, 11 mi E Nuevo Laredo (KU 89054); (27) Tamaulipas: 9.5 mi SW Padilla (KU 88544); (28) Tamaulipas: Ciudad Victoria (USNM 93350); (29) Zacatecas: 5.5 km NW Juan Aldama (OMNH 9981); (30) Zacatecas: Valparaíso (**USNM 91874, USNM 91875, USNM 91876, USNM 91878, USNM 91879, USNM 91880, USNM 91881, USNM 91882**); (31) Zacatecas: 8 mi SE Zacatecas (KU 48666, KU 48667, KU 49007). UNITED STATES. (32) Texas: Aransas Co., Aransas Refuge (TCWC 1833); (33) Texas: Bexar Co., 5 mi S McConnell, 5.3 mi E Lytle, FM 2790 (TCWC 27596); (34) Texas: Cameron Co., Harlingen, 5.2 mi E US Business 77 on FM 106 (TCWC 38671); (35) Texas: Colorado Co., 9 mi E Eagle Lake (TCWC 874); (36) Texas: Dimmit Co., 2 mi SW Asherton, Hwy 1916 (TCWC 27597); (37) Texas: Dimmit Co., 10 mi SW Carrizo Springs (TCWC 27978); (38) Texas: Frio Co., 3 mi S, 3.5 mi W Pearsall (TCWC 34764); (39) Texas: Frio Co., 3 mi S Pearsall (TCWC 39513); (40) Texas: Frio Co., 1.1 mi NW Pearsall on FM 140 (TCWC 50374); (41) Texas: Hidalgo Co., 2 mi S, 2.75 mi E Hidalgo (TCWC 44084); (42) Texas: Jim Hogg Co., 18 mi Hebbronville on Hwy 16 (TCWC 28651); (43) Texas: Jim Hogg Co., 5.3 mi S junction of Hwys 3073 and 649, on Hwy 649 (TCWC 29712); (44) Texas: Jim Hogg Co., 13.4 mi SSE Mirando City on Hwy 649 (TCWC 29716); (45) Texas: Jim Wells Co., 4 mi S, 7 mi W Alice (TCWC 43668); (46) Texas: Karnes Co., 1.75 mi N, 3.5 mi E Kenedy (TCWC 43678); (47) Texas: Kleberg Co., 2 mi S Riviera (TCWC 2584); (48) Texas: La Salle Co., 35 mi SE Cotulla (TCWC 1326); (49) Texas: La Salle Co., 2 mi S Woodward (TCWC 1327); (50) Texas: La Salle Co., 8 mi NE Los Angeles (TCWC 1376); (51)

Texas: Maverick Co., 1.5 mi N, 4.5 mi E Eagle Pass (TCWC 44086); (52) Texas: Maverick Co., 12 mi S, 6 mi E Spofford (TCWC 44087); (53) Texas: San Patricio Co., 3.5 mi S, 2 mi W Mathis (TCWC 43687); (54) Texas: Webb Co., 4.5 mi SSE Mirando City on Hwy 649 (TCWC 29715); (55) Texas: Webb Co., 18 mi N, 4.5 mi E Oilton, Gates Lake Area (TCWC 44098); (56) Texas: Willacy Co., La Sal Vieja, about 6 mi W US 77, SE side eastern lake on FM 1761 (TCWC 38670); (57) Texas: Willacy Co., Red Fish Bay, 28 mi E Raymondville (TCWC 2588); (58) Texas: Willacy Co., 7 mi N, 4.5 mi W Raymondville (TCWC 41549); (59) Texas: Willacy Co., 6 mi N Raymondville (TCWC 43690); (60) Texas: Zapata Co., Swantner-Hunter Ranch, 1 mi NE Zapata (TCWC 34828); (61) Texas: Zapata Co., 4 mi N, 4 mi W Zapata (TCWC 43691); (62) Texas: Zapata Co., 9 mi S Batesville, Paysinger Ranch (TCWC 44102).

Chaetodipus hispidus conditi (n = 20).—MÉXICO. (63) Chihuahua: Casas Grandes (USNM 97376, USNM 97384); (64) Chihuahua: 5 mi N El Carmen (KU 85949); (65) Chihuahua: 1.5 mi E General Trias (KU 69776); (66) Chihuahua: Presa Colina, 10.5 km NW La Boquilla (OMNH 10683); (67) Chihuahua: 1.5 mi N San Francisco (KU 69775); (68) Chihuahua: 4 mi NW San Francisco De Borja (KU 82461, KU 82463); (69) Chihuahua: Santa Rosalia (USNM 56257); (70) Chihuahua: Estación Arados (KU 66592).

UNITED STATES. (71) Arizona: Cochise Co., Chiricahua Mountains, Mouth of Turkey Creek (USNM 247489, USNM 248006); (72) Arizona: Cochise Co., Huachuca Mountains (USNM 21506, USNM 21508); (73) Arizona: Santa Cruz Co., Santa Cruz River, W Patagonia Mountains (USNM 21505); (74) New Mexico: Grant Co., Gila (USNM 158651); (75) New Mexico: Grant Co., Redrock (USNM 158650); (76) New Mexico: Hidalgo Co., 22.7 mi S, 4.2 mi W Animas (OMNH 7771, OMNH 7773); (77) New Mexico: Hidalgo Co., 0.3 mi N Cloverdale (USNM 349386).

Chaetodipus hispidus paradoxus (n = 203).—UNITED STATES. (78) Colorado: Adams Co., 3 mi S, 1 mi W Simpson (KU 74667); (79) Colorado: Boulder Co. (USNM 192256); (80) Colorado: Cheyenne Co., 5 mi SW Kit Carson (USNM 513393); (81) Colorado: Huerfano Co., 1 mi S, 2 mi W Walsenburg (KU 121011); (82) Colorado: Logan Co., Sterling (USNM 35112); (83) Colorado: Kit Carson Co., 3 mi NE Burlington (KU 87751); (84) Colorado: Washington Co., Cope (KU 74668); (85) Kansas: Barber Co., 6 mi N Aetna (KU 11981); (86) Kansas: Barber Co., Plum Thicket, Sharon (KU 60163); (87) Kansas: Barber Co., 5 mi N, 0.5 mi E Sharon (KU 99263); (88) Kansas: Barber Co., 2 mi N, 0.5 mi E Sharon (KU 99264); (89) Kansas: Barber Co., Barber County State Lake, 1 mi N Medicine Lodge (KU 136237); (90) Kansas: Barber Co., 2.5 mi S, 1 mi W Medicine Lodge (KU 109609, KU 109611, KU 135846); (91) Kansas: Barton Co., 2 mi N, 2 mi W Hoisington (KU 16277, KU 16278); (92) Kansas: Chase Co., 2 mi W Cottonwood Falls (KU 12214); (93) Kansas: Chautauqua Co., 4 mi S Cedar Vale (KU 136009); (94) Kansas: Clark Co., E A Stephenson Ranch, 7 mi SW Kingsdown (KU 11704); (95) Kansas: Cloud Co., Bulock Farm, 1 mi N, 3.5 mi E Glasco (KU 29363); (96) Kansas: Cloud Co., 3 mi S, 1 mi E St. Joseph (KU 102919, KU 102920, KU 102925, KU 102932); (97) Kansas: Comanche Co., Swartz Canyon (KU 69494); (98) Kansas: Cowley Co., Arkansas City (KU 5066); (99) Kansas: Cowley Co., 8.6 mi E Arkansas City (KU 39263); (100) Kansas: Cowley Co., 5 mi W Winfield (KU 160077); (101) Kansas: Ellsworth Co., 1.5 mi S Wilson (KU 14052); (102) Kansas: Ford Co., Dodge City, 1 mi S, 5 mi W of Courthouse (KU 100152); (103) Kansas: Ford Co., 3 mi SW Dodge City (KU 119248, KU 139026); (104) Kansas: Greenwood Co., Hamilton (KU 52963); (105) Kansas: Greenwood Co., 0.25 mi S Hamilton (KU 52967); (106) Kansas: Greenwood Co., 8.5 mi SW Toronto (KU 8649); (107) Kansas: Hamilton Co., 1 mi E Coolidge (KU 11706); (108) Kansas: Harper Co., 4.5 mi NE Danville (KU 13043); (109) Kansas: Harper Co., 5 mi NW Harper (KU 13536, KU 13539); (110) Kansas: Harvey Co., 8 mi W Newton (KU 4031); (111) Kansas: Kiowa Co., SE corner of Kiowa Co. (KU 13880); (112) Kansas: Lane Co., Pendennis (KU 21005); (113) Kansas: Lyon Co., 2 mi S Chalk (KU 38834); (114) Kansas: Marion Co., 0.5 mi E Lincolnville (KU 11710); (115) Kansas: Meade Co., Meade State Park (KU 11705); (116) Kansas: Meade Co., Meade State Park, 14 mi SW Meade (KU 52954); (117) Kansas: Meade Co., 17 mi SW Meade (KU 13772, KU 14047); (118) Kansas: Mitchell Co., 0.5 mi S, 3.5 mi W Beloit (KU 20361); (119) Kansas: Morris Co., 4.125 mi S, 6 mi W Council Grove (KU 99262); (120) Kansas: Morton Co., 8 mi N Elkhart (KU 38833, KU 100153); (121) Kansas: Norton Co., 1 mi S, 4 mi W Logan (KU 18843); (122) Kansas: Pawnee Co., 1 mi S Larned (KU 16283); (123) Kansas: Pratt Co., 4 mi S, 0.5 mi W Cairo (KU 143929); (124) Kansas: Rawlins Co., 6 mi S Atwood (KU 35092); (125) Kansas: Reno Co., Turon (KU 63219); (126) Kansas: Republic Co., Rydal (KU 74685, KU 74686); (127) Kansas: Riley Co., Camp Forsyth (TCWC 50378, TCWC 50381); (128) Kansas: Seward Co., 3 mi NE Liberal (KU 76323); (129) Kansas: Sheridan Co., 15 mi S, 15 mi E Hoxie (KU 113807, KU 113808, KU 113813); (130) Kansas: Smith Co., 6 mi S Smith Center (KU 63217); (131) Kansas: Stanton Co., 1.5 mi N, 6 mi W Manter (KU 38829); (132) Kansas: Thomas Co., Colby (USNM 54450); (133) Kansas: Trego Co. (USNM 192257); (134) Kansas: Trego Co., Banner (**USNM 186513**); (135) Kansas: Washington Co., Washington State Fishing Lake, 7.75 mi N, 3 mi W Washington (KU 139195); (136) Kansas: Wichita Co., Marienthal, 15 mi W Scott City (KU 55624, KU 55626, KU 55630, KU 55633); (137) Louisiana: Vernon Parish: Red Leg Impact Area, Fort Polk (USNM 569153); (138) Montana: Carter Co., 5 mi N, 3.5 mi W Camp Crook (KU 123378); (139) Nebraska: Banner Co., 7.5 mi N, 1 mi E Harrisburg (KU 80955); (140) Nebraska: Cass Co., 2 mi N, 2 mi W Weeping Water (KU 115936); (141) Nebraska: Cherry Co. (USNM 16931); (142) Nebraska: Cherry Co., 4 mi E Valentine (KU 73272); (143) Nebraska: Cheyenne Co., 15 mi S Dalton (KU 15280); (144) Nebraska: Custer Co., Myrtle P.O. (USNM 16719); (145) Nebraska: Dawes Co., 3 mi E Chadron (KU 50138); (146) Nebraska: Deuel Co., 1 mi N, 2 mi W Chappell (KU 57272); (147) Nebraska: Franklin Co., 1.5 mi S Franklin (KU 74674); (148) Nebraska: Gage Co., 1 mi S, 1 mi W Barnston (KU 72058); (149) Nebraska: Gage Co., 1.5 mi S, 2 mi E Barnston (KU 74430); (150) Nebraska: Kimball Co., Smeed (KU 76931); (151) Nebraska: Otoe Co., 3 mi S, 2 mi E

Nebraska City (KU 55241); (152) Nebraska: Pawnee Co., 4 mi S, 8 mi W Pawnee City (KU 72061); (153) Nebraska: Richardson Co., 4 mi E Barada (KU 72066, KU 72067); (154) Nebraska: Richardson Co., 3 mi S Rulo (KU 74690); (155) Nebraska: Scotts Bluff Co., 10 mi S Scotts Bluff (KU 15278); (156) Nebraska: Scotts Bluff Co., 11 mi S Scottsbluff (KU 15279); (157) Nebraska: Sioux Co., 6.5 mi W Crawford (KU 73269); (158) Nebraska: Webster Co., Red Cloud (USNM 54750); (159) New Mexico: Chaves Co., Roswell (USNM 96360); (160) New Mexico: Otero Co., Tularosa (USNM 119115); (161) New Mexico: Roosevelt Co., 9 mi S, 1 mi W Tolar (KU 166726, OMNH 5333); (162) New Mexico: San Miguel Co., Las Vegas (USNM 64601); (163) New Mexico: Socorro Co., Dry Creek (USNM 158654); (164) Oklahoma: Beaver Co., Beaver River Wildlife Management Area, 3.9 mi S, 4 mi W Floris (OMNH 29879); (165) Oklahoma: Beckham Co., Sandy Sanders Wildlife Management Area, 11.75 mi S, 2.25 mi E Erick (OMNH 29842); (166) Oklahoma: Blaine Co., 1 mi N Hydro (KU 43876); (167) Oklahoma: Caddo Co., 10 mi NE Binger (OMNH 19273); (168) Oklahoma: Cimarron Co., Black Mesa (OMNH 4511); (169) Oklahoma: Cimarron Co., Near Lake Etling, 20 mi NW Boise City (OMNH 19274); (170) Oklahoma: Cimarron Co., 4.6 mi N, 0.2 mi W Kenton (KU 166727); (171) Oklahoma: Cleveland Co., 6 mi E Norman (OMNH 18999); (172) Oklahoma: Cleveland Co., 12 mi E Norman (OMNH 14930); (173) Oklahoma: Comanche Co., Fort Sill Game Farm (USNM 273757); (174) Oklahoma: Comanche Co., Fort Sill, 6.5 mi S Elgin (OMNH 19525); (175) Oklahoma: Comanche Co., Lawton (USNM 139281); (176) Oklahoma: Comanche Co., Mount Scott P.O. near Cache Creek (USNM 132567); (177) Oklahoma: Comanche Co., Wichita Mountains Wildlife Refuge Little Medicine Creek (USNM 273759); (178) Oklahoma: Comanche Co., Wichita Mountains Wildlife Refuge Meck's Juniper Plantation (USNM 273761); (179) Oklahoma: Comanche/Tillman Co., Chattanooga (USNM 137485); (180) Oklahoma: Cotton Co., 5 mi S Taylor (OMNH 2447); (181) Oklahoma: Custer Co., T13N, R20W (OMNH 16953); (182) Oklahoma: Custer Co., 6 mi W Weatherford (KU 45196); (183) Oklahoma: Dewey Co., 5.5 mi SW Canton (KU 10200); (184) Oklahoma: Dewey Co., 5 mi W Canton (KU 12407, KU 43859); (185) Oklahoma: Dewey Co., 1 mi N Taloga (OMNH 3914); (186) Oklahoma: Ellis Co., Packsaddle Wildlife Management Area, 11 mi S, 3 mi E Arnett (OMNH 29798); (187) Oklahoma: Grady Co., Alex (OMNH 7232); (188) Oklahoma: Greer Co., 3 mi E Reed (OMNH 4231); (189) Oklahoma: Harmon Co., 2 mi S, 2 mi W Reed (KU 119500); (190) Oklahoma: Harmon Co., 1 mi S, 6 mi E Vinson (OMNH 2434); (191) Oklahoma: Harper Co., 3 mi N Fort Supply (USNM 272162, USNM 272168, USNM 273217); (192) Oklahoma: Harper Co., Southern Plains Exp. Range, 3 mi NWN Supply (USNM 272602); (193) Oklahoma: Indian Territory, 8 mi W Red Fork (USNM 133138); (194) Oklahoma: Haskell Co., 1.5 mi E Porum (OMNH 13963); (195) Oklahoma: Johnston Co. 0.5 mi NE Headquarters, Tishomingo National Wildlife Refuge (USNM 289003); (196) Oklahoma: Kay Co., 5 mi S, 7 mi E Newkirk (OMNH 8728); (197) Oklahoma: Le Flore Co., 5 mi N, 2.5 mi E Bokoshe (OMNH 13980); (198) Oklahoma: Logan Co., T16N, R4W (OMNH 169); (199) Oklahoma: Logan/Payne Co., Orlando (USNM 35274); (200) Oklahoma: Major Co., Whitlaw Ranch Vickery #1 Cave, 1 mi SW junction Hwys 15 and 281 (OMNH 19277); (201) Oklahoma: Marshall Co., Lake Texoma Fobb Bottom sand dunes, University of Oklahoma Biological Station (OMNH 15493); (202) Oklahoma: Marshall Co., 1 mi W Willis (OMNH 941); (203) Oklahoma: McClain Co., 5.6 mi S, 2 mi W Washington (OMNH 32504); (204) Oklahoma: Muskogee Co., 3 mi E Wainwright (OMNH 5548); (205) Oklahoma: Roger Mills Co., 7 mi N Cheyenne (OMNH 760); (206) Oklahoma: Rogers Co., Garnett (USNM 293446); (207) Oklahoma: Tillman Co., 0.5 mi W Chattanooga (OMNH 3486); (208) Oklahoma: Wagoner Co., 2.5 mi SSW Coweta (OMNH 2935); (209) Oklahoma: Woods Co., Alva (USNM 96064); (210) Oklahoma: Woods Co., 5 mi NW Alva (KU 81885); (211) Oklahoma: Woods Co., 8.5 mi NW Alva (OMNH 10871); (212) Oklahoma: Woods Co., 5 mi S Waynoka (OMNH 3292); (213) South Dakota: Bennett Co., Lacreek National Wildlife Refuge, 4 mi S, 8 mi E Martin (KU 113108, KU 113109); (214) South Dakota: Buffalo Co., 2 mi S, 3 mi E Fort Thompson (KU 41900); (215) South Dakota: Custer Co., Elk Mountain, Campbell's Ranch (USNM 130849); (216) South Dakota: Custer Co., Wind Cave National Park, Wind Cave Canyon (KU 116406); (217) South Dakota: Custer Co., Wind Cave National Park, 6 mi N, 1 mi E Wind Cave (KU 112560); (218) South Dakota: Fall River Co., 0.5 mi S, 1.5 mi W Minnekahta (KU 113107); (219) South Dakota: Harding Co., 14 mi S, 4 mi W Reva (KU 86443); (220) South Dakota: Jackson Co., 1 mi S, 2 mi E Cottonwood (KU 128339); (221) South Dakota: Mellette Co., Galbraith (KU 159192); (222) South Dakota: Sully Co., Koenig GPA (KU 159193); (223) South Dakota: Walworth Co., Swan Creek, 13 mi S Selby (KU 37166); (224) Texas: Brazos Co., 7 mi SW College Station (TCWC 23395); (225) Texas: Brazos Co., 2 mi W College Station (TCWC 23398); (226) Texas: Brazos Co., College Station, 0.6 mi N junction 60 and 2818 (TCWC 30324); (227) Texas: Caldwell Co., 3 mi NW Lytton Springs (TCWC 31906); (228) Texas: Clay Co., 3 mi SE Henrietta (TCWC 1893); (229) Texas: Cooke Co., Gainesville (USNM 35933); (230) Texas: Coryell Co., Fort Hood, 12.2 mi NNE Copperas Cove (TCWC 58372); (231) Texas: Fisher Co., 1 mi S Rody on Hwy 70 (TCWC 30326); (232) Texas: Hemphill Co., 6 mi E Canadian, Gene Howe Area (TCWC 5787); (233) Texas: Hill Co., 2 mi S, 0.5 mi W Hillsboro (TCWC 38214); (234) Texas: Hill Co., 3.1 mi S, 6.6 mi W Hillsboro (TCWC 38216); (235) Texas: Hill Co., 3.6 mi S, 6.9 mi W Hillsboro (TCWC 38633); (236) Texas: Hill Co., 3.4 mi S, 5.1 mi W Hillsboro (TCWC 38220); (237) Texas: Hill Co., 3.6 mi S, 6.9 mi W Hillsboro (TCWC 38223); (238) Texas: Hill Co., 5.8 mi S, 3.1 mi W Hillsboro (TCWC 38231); (239) Texas: Hutchinson Co., 1 mi S, 10 mi E Pringle (KU 119497); (240) Texas: Kerr Co., 20 mi W Mountain Home (TCWC 313); (241) Texas: Kerr Co., 4 mi NE Center Point (TCWC 335); (242) Texas: Kerr Co., Kerrville, Hwy near State Park

(TCWC 3528); (243) Texas: Kimble Co., Junction (TCWC 28648); (244) Texas: Madison Co., 1 mi S junction Hwys 21 and I-45 (TCWC 30323); (245) Texas: Robertson Co., 5 mi SE Hearne (TCWC 34383); (246) Texas: Smith Co., 4 mi N Tyler (TCWC 3732); (247) Texas: Tom Green Co., 6.5 mi SW San Angelo, near Twin Buttes Reservoir (TCWC 30327, TCWC 30328); (248) Texas: Val Verde Co., Long Point, Amistad National Recreation Area (TCWC 31157); (249) Texas: Wichita Co., 11.5 mi N Wichita Falls (KU 114431); (250) Texas: Wilbarger Co., 20.8 mi S Vernon (OMNH 6821); (251) Wyoming: Crook Co., 2 mi N, 14 mi W Hulett (KU 32462); (252) Wyoming: Laramie Co., Horse Creek, 6.5 mi W Meriden (KU 15276); (253) Wyoming: Laramie Co., 2 mi S Pine Bluffs (KU 25673); (254) Wyoming: Platte Co., 2.5 mi S Chugwater (KU 18252, KU 18254, KU 18257).

Appendix III

List of newly designed internal forward (F) and reverse (R) primers for cytochrome *b* (*Cytb*) and reduced nicotinamide adenine dinucleotide dehydrogenase 2 (ND2) used for amplification and sequencing of museum skin snip specimens of *Chaetodipus hispidus*. Fragment length varied from 163 to 396 base pairs (bp) in *Cytb* and 296 to 655 bp in ND2.

Gene	Strand	Primer name	Sequence (5′–3′)
Cytb	F	CHcytbF2	CAC GCA TTT ATT GAC CTG CCA
	R	CHcytbR2	GRG CTA CTG ATG AGA ATG CTG T
	F	CHcytbF3	TTA TCC WAA TTK CTT CAG GAC T
	R	CHcytR3	ARC CAT AAT AAA TCC YTC GGC
	F	CHcytbF4	YAT YCA CGC WAA TGG AGC TTC
ND2	F	CHnd2F2	YAR CCC ACG ATC TAC AGA AG
	R	CHnd2R2	GRG TTA CTT CAG GRA CTC AGA
	F	CHnd2F3	ACC AGA AGA YAT RYT ATC CCA AT
	R	CHnd2R3	CCY CAK CCT CCT AGA AKA AT
	F	CHnd2F4	AAR TCA GGR CTA ATT CTT CTC AC
	R	CHnd2R4	TAA GYT ACG ATA GCT GAY ATT CA
	F	CHnd2F5	TYA TAG CAT AYT CAT CTA TTG CCC
	R	CHnd2R5	GTR GCR TTA GTR TTY CAT GC
	F	CHnd2F6	TGC CCT YAC YAY AAC AAT ATT TT
	R	CHnd2R6	GCT ATA ATR AGG CTR ACT AGR AT

Appendix IV

Best models of evolution for cytochrome oxidase subunit III (COIII), cytochrome *b* (*Cytb*), and reduced nicotinamide adenine dinucleotide dehydrogenase 2 (ND2) for each data set for *Chaetodipus hispidus* as determined by ModelTest (version 3.6—Posada and Crandall 1998) and MrModeltest (version 2.3—Nylander et al. 2004).

Data set	ModelTest	MrModeltest
Fresh tissue samples only (47 ingroup taxa)		
COIII	TVM+I+G	GTR+I+G
1st codon position		SYM+I
2nd codon position		GTR
1st + 2nd codon positions		GTR+I
3rd codon position		GTR+G
Cytb	GTR+I+G	GTR+G
1st codon position		HKY+G
2nd codon position		HKY
1st + 2nd codon positions		HKY+G
3rd codon position		HKY+G
ND2	TVM+G	HKY+G
1st codon position		GTR+I
2nd codon position		GTR+I+G
1st + 2nd codon positions		GTR+I+G
3rd codon position		GTR+I
Combined 3 genes	HKY+I+G	HKY+I+G
1st codon position		GTR+I
2nd codon position		HKY
1st + 2nd codon positions		HKY+G
3rd codon position		GTR+G
Fresh tissue samples and museum skin snips (63 ingroup taxa)		
Cytb	HKY+G	GTR+I+G
1st codon position		GTR+G
2nd codon position		F81+I
1st + 2nd codon positions		GTR+G
3rd codon position		HKY+G
ND2	HKY+I+G	GTR+I+G
1st codon position		GTR
2nd codon position		GTR+G
1st + 2nd codon positions		GTR+I+G
3rd codon position		GTR+I
Combined 2 genes	TrN+I+G	HKY+I+G
1st codon position		GTR+I
2nd codon position		GTR+G
1st + 2nd codon positions		GTR+I
3rd codon position		GTR+I+G
Combined 3 genes	HKY+I+G	GTR+I+G
1st codon position		GTR+G
2nd codon position		GTR+G
1st + 2nd codon positions		GTR+I+G
3rd codon position		GTR+I+G